

# Emanant and emergent symmetry-topological-order from low-energy spectrum

Zixin Jessie Chen,<sup>1</sup> Ömer M. Aksoy,<sup>1</sup> Cenke Xu,<sup>2</sup> and Xiao-Gang Wen<sup>1</sup>

<sup>1</sup>*Department of Physics, Massachusetts Institute of Technology, Cambridge, Massachusetts 02139, USA*

<sup>2</sup>*Department of Physics, University of California, Santa Barbara, CA 93106, USA*

Low-energy emergent and emanant symmetries can be anomalous, higher-group, or non-invertible. Such symmetries are systematically captured by topological orders in one higher dimension, known as symmetry topological orders (symTOs). Consequently, identifying the emergent or emanant symmetry of a system is not simply a matter of determining its group structure, but rather of computing the corresponding symTO. In this work, we develop a method to compute the symTO of 1+1D systems by analyzing their low-energy spectra under closed boundary conditions with all possible symmetry twists. Applying this approach, we show that the gapless antiferromagnetic (AF) spin- $\frac{1}{2}$  Heisenberg model possesses an exact emanant symTO corresponding to the  $D_8$  quantum double, when restricted to the  $\mathbb{Z}_2^x \times \mathbb{Z}_2^z$  subgroup of the  $SO(3)$  spin-rotation symmetry and lattice translations. Moreover, the AF phase exhibits an emergent  $SO(4)$  symmetry, whose exact components are described jointly by the symTO and the  $SO(3)$  spin-rotations. Using condensable algebras in symTO, we further identify several neighboring phases accessible by modifying interactions among low-energy excitations: (1) a gapped dimer phase, connected to the AF phase via an  $SO(4)$  rotation, (2) a commensurate collinear ferromagnetic phase that breaks translation by one site with a  $\omega \sim k^2$  mode, (3) an incommensurate, translation-symmetric ferromagnetic phase featuring both  $\omega \sim k^2$  and  $\omega \sim k$  modes, connected to the previous phase by an  $SO(4)$  rotation, and (4) an incommensurate ferromagnetic phase that breaks translation by one site with both  $\omega \sim k^2$  and  $\omega \sim k$  modes.

## CONTENTS

		A. $S$ -matrix and fusion rules of $D_8$ quantum double $\mathcal{D}(D_8)$	22
		References	24
I. Introduction	1		
II. Heisenberg model and its phase diagram	3		
A. Definitions and symmetries	3		
B. Adjacent gapped phases	3		
III. Low-energy excitations from exact diagonalization	4		
A. The spectrum calculation	6		
B. The spectra for PBC	7		
C. The spectra for TBC	8		
D. Emanant symmetries and anomalies	9		
IV. Identifying SymTO $\mathcal{D}(D_8)$ from sectors of low-energy spectra	10		
A. Charge sectors	10		
B. Flux sectors	12		
1. Fluxes and dyons for $\mathbb{Z}_2^z$ and $\mathbb{Z}_2^t$ symmetry twists	12		
2. Fluxes and dyons for pure translation symmetry twists	13		
C. Matching with SymTO $\mathcal{D}(D_8)$	14		
V. SymTO $\mathcal{D}(D_8)$ and nearby gapped phases	14		
A. $D_8$ quantum double $\mathcal{D}(D_8)$	14		
VI. $SO(4)$ representation of 2d SPT and its connection to 1d Spin Chain	17		
VII. Gapless CFT boundary of symTO $\mathcal{D}(D_8)$	18		
VIII. Neighboring states of spin- $\frac{1}{2}$ Heisenberg chain	19		
IX. Conclusion & Outlook	21		
Acknowledgments	21		

## I. INTRODUCTION

Symmetry is one of the most important properties of a physical system: it constrains low-energy behavior, nearby phases, and the transitions between them. The low-energy effective theory of a lattice model may exhibit both *emanant* symmetry and *emergent* symmetry [1]. The emanant symmetry originates from the original exact lattice symmetry, which can take a very different form in the low-energy effective theory; the emergent symmetry is an additional symmetry that is present only at low energies. In recent years, it has become clear that emergent and emanant symmetries can be very general [2–4]: they can combine ordinary (0-form) symmetries (described by groups), higher-form and higher-group symmetries [5–8], anomalous ordinary symmetries [2, 9–13], anomalous higher symmetries [7, 8, 14–23], non-invertible 0-form symmetries (in 1+1D) [24–35], non-invertible higher (“algebraic higher”) symmetries [36–42], and/or non-invertible gravitational anomalies [43–48], including anomaly-free/anomalous non-invertible higher symmetries described by fusion higher categories [36, 37, 42, 49]. These generalized symmetries go beyond groups, and even beyond higher groups and standard anomaly notions, yet they can all be described by topological orders in one higher dimension. In fact, topological orders with a gapped boundary classify all finite generalized symmetries (up to holomorphic equivalence [37, 49], also known as Morita equivalence) in

one lower dimension. We therefore refer to such bulk data as *symmetry-topological order* (symTO) or *symmetry-topological field theory* (symTFT).

A connection between boundary symmetry and bulk topological order was first observed in Ref. 50, where the topological entanglement entropy was shown to originate from a boundary conservation law rooted in the bulk topological order; this was later confirmed numerically [51]. A systematic symmetry/topological-order correspondence was developed via the holographic picture of emergent non-invertible gravitational anomalies [46, 48, 52] and of dualities [53, 54], leading to a holographic understanding of generalized symmetries [37, 42, 49, 55–58]. This holographic point of view has been applied to understand gapped and gapless phases of matter with generalized symmetries [32, 37, 59–79].

With this classification-oriented viewpoint, determining a system's low-energy emergent or emanant symmetry is no longer just a computation of a group structure. Instead, one needs to identify the corresponding symTO in one higher dimension. This requires a new type of calculation and is the main focus of this paper. As an illustrative example, we study the spin- $\frac{1}{2}$  antiferromagnetic Heisenberg chain with  $SO(3)$  spin-rotation and translation symmetries, and compute its low-energy symTO (equivalently, the associated braided tensor category).

Because the symTO for the continuous spin-rotation symmetry  $SO(3)$  is not yet fully developed, we first tackle a simpler problem by reducing the spin rotations to the  $\mathbb{Z}_2^x$ ,  $\mathbb{Z}_2^y$ , and  $\mathbb{Z}_2^z$  symmetries generated by  $\pi$ -rotations about  $S_x, S_y, S_z$ . Thus we consider the spin- $\frac{1}{2}$  XYZ model with translation symmetry near the isotropic limit:

$$H = \sum_{j=1}^L (J_x S_j^x S_{j+1}^x + J_y S_j^y S_{j+1}^y + J_z S_j^z S_{j+1}^z), \quad (1)$$

with  $J_x, J_y, J_z \sim 1$  (i.e.  $|J_x - J_y|, |J_y - J_z|, |J_x - J_z| \ll J_x, J_y, J_z$ ). The lattice symmetry of the XYZ model is  $\mathbb{Z}_2^x \times \mathbb{Z}_2^y \times \mathbb{Z}_L$ , where  $\mathbb{Z}_L$  denotes translations.

We compute the low-energy emanant symmetry at energies  $\ll J_x, J_y, J_z \sim 1$ . The emanant symmetry includes the spin-rotation subgroup  $\mathbb{Z}_2^x \times \mathbb{Z}_2^y$  and the translation symmetry  $\mathbb{Z}_2^t$ . The lattice translation  $\mathbb{Z}_L$  reduces to  $\mathbb{Z}_2^t$  emanant symmetry because translation by two lattice spacing acts trivially on the ground states when  $J_x, J_y, J_z \sim 1$ . However, the emanant symmetry is not simply  $\mathbb{Z}_2^x \times \mathbb{Z}_2^y \times \mathbb{Z}_2^t$ . Instead, we find that the combined symmetry is encoded by the symTO of the  $D_8$  quantum double,  $\mathcal{D}(D_8)$ . This conclusion follows from the low-energy spectra of the model under various symmetry-twist boundary conditions. Our method for extracting symTO from low-energy spectra is general and applies to other 1+1D system.

What does it mean for the low-energy effective theory of the XYZ model to have an exact symmetry described by the symTO  $\mathcal{D}(D_8)$ ? A useful viewpoint is that a symTO corresponds to a collection of symmetries which

form a holo-equivalence class. The low-energy dynamics is constrained by every symmetry in this class. The holo-equivalence class of  $\mathcal{D}(D_8)$  contains a  $\mathbb{Z}_2^x \times \mathbb{Z}_2^y \times \mathbb{Z}_2^{zt}$  symmetry with a type-III mixed anomaly (here  $\mathbb{Z}_2^{zt}$  is generated by the combined action of  $\mathbb{Z}_2^z$  and  $\mathbb{Z}_2^t$ ). Therefore, the emanant symmetry of the XYZ model is  $\mathbb{Z}_2^x \times \mathbb{Z}_2^y \times \mathbb{Z}_2^{zt}$  with a type-III mixed anomaly.

The holo-equivalence class also contains a  $D_8$  symmetry, which constrains the low-energy dynamics of the XYZ model. Thus, in some sense,  $D_8$  can also be regarded as an emanant symmetry of the XYZ model. However, some  $D_8$  charges may correspond to non-local excitations in the XYZ model.

Although the emanant symmetry of the XYZ chain can be described by a group with an anomaly, the holographic  $\mathcal{D}(D_8)$  symTO point of view is still very useful. It allows us to use the Lagrangian condensable algebras of  $\mathcal{D}(D_8)$  to systematically obtain all possible gapped phases for systems with the symTO. We find that there are only 11 possible gapped phases for nearly isotropic XYZ chain.

The spin- $\frac{1}{2}$   $SO(3)$ -symmetric Heisenberg chain also exhibits the emanant symTO  $\mathcal{D}(D_8)$  at low energies. We identify an  $S_3$  subgroup of the  $S_4$  automorphism group of  $\mathcal{D}(D_8)$  that permutes the  $\mathbb{Z}_2^x$ ,  $\mathbb{Z}_2^y$ , and  $\mathbb{Z}_2^z$  symmetries contained in  $\mathcal{D}(D_8)$ . Consequently, this  $S_3$  automorphism is a part of  $SO(3)$  rotation and becomes an emanant symmetry of the  $SO(3)$ -symmetric Heisenberg chain.

The full  $S_4$  automorphism is not an emanant symmetry of the Heisenberg chain. However, it emerges as an approximate symmetry that becomes increasingly accurate at lower energies. Combining the exact  $SO(3)$  spin-rotation symmetry with this emergent  $S_4$ , one obtains an emergent anomalous  $SO(4)$  symmetry for the  $SO(3)$  Heisenberg chain, a well-known result [80, 81]. Such an emergent anomalous  $SO(4)$  symmetry should contain the anomaly-free emanant  $SO(3)$  spin-rotation symmetry together with the emanant symTO  $\mathcal{D}(D_8)$ . Since  $\mathcal{D}(D_8)$  can be viewed as  $\mathbb{Z}_2^x \times \mathbb{Z}_2^y \times \mathbb{Z}_2^{zt}$  with a type-III mixed anomaly, this suggests that

the full emanant symmetry of the  $SO(3)$  Heisenberg chain is  $SO(3) \times \mathbb{Z}_2^t$  with a mixed anomaly. Such an emanant symmetry is the exact part of the emergent anomalous  $SO(4)$  symmetry.

We remark that, *a priori*, the emanant symmetry could go beyond anomalous symmetries; our calculations indicate, however, that it lies within the anomalous class and is naturally  $SO(3) \times \mathbb{Z}_2^t$  with a mixed anomaly.

How are the anomalies in the emergent  $SO(4)$  and in the emanant  $SO(3) \times \mathbb{Z}_2^t$  related? We regard  $SO(4)$  as  $(SU_R(2) \times SU_L(2))/\mathbb{Z}_2$ , whose anomaly is characterized by a cocycle in  $H^3(SO(4); \mathbb{R}/\mathbb{Z}) = H^3(SU_L(2) \times SU_R(2); \mathbb{R}/\mathbb{Z}) = \mathbb{Z}_L \times \mathbb{Z}_R$ . Thus  $SO(4)$  anomalies are labeled by  $(k_L, k_R) \in \mathbb{Z}^2$ . The  $SO(3) \times \mathbb{Z}_2^t$  anomaly lies in  $H^3(SO(3) \times \mathbb{Z}_2^t; \mathbb{R}/\mathbb{Z}) = \mathbb{Z} \times \mathbb{Z}_2$ , where the  $\mathbb{Z}_2$  factor records the mixed anomaly; accordingly we label these anomalies by  $(k, \sigma) \in \mathbb{Z} \times \mathbb{Z}_2$ . Under restriction, an  $SO(4)$

anomaly  $(k_R, k_L)$  reduces to an  $SO(3) \times \mathbb{Z}_2^t$  anomaly

$$(k, \sigma) = (k_R + k_L, k_R \pmod{2}).$$

In our case, the anomaly of emergent  $SO(4)$  is  $(k_R, k_L) = (1, -1)$ , which gives rise to the  $su_{21} \times su_{21}$  Kac-Moody algebra describing decoupled gapless right-movers and left-movers in the  $SO(3)$  Heisenberg chain. This  $SO(4)$  anomaly reduces to an  $SO(3) \times \mathbb{Z}_2^t$  anomaly ( $k = 0, \sigma = 1$ ). The  $SO(3)$  Heisenberg chain can also be described by a  $(1+1)D$  nonlinear sigma model defined in  $S^2$  with a topological  $\Theta$ -term, and the  $\mathbb{Z}_2$  nature of  $\sigma$  corresponds to the two symmetric choices  $\Theta = 0, \pi$ .

An important application of these emanant and emergent symmetries is to constrain phases neighboring the gapless phase of the Heisenberg chain. Knowing the symTO of the emanant and emergent symmetry allows us to employ condensable algebras of the symTO to obtain these neighboring gapped and gapless phases, which is done in Sections V and VIII.

## II. HEISENBERG MODEL AND ITS PHASE DIAGRAM

### A. Definitions and symmetries

We consider the quantum spin-1/2 antiferromagnetic Heisenberg chain

$$H = \sum_{j=1}^L \mathbf{S}_j \cdot \mathbf{S}_{j+1}, \quad (2a)$$

where the components  $\mathbf{S}_j = (S_j^x, S_j^y, S_j^z)$  satisfy the algebra

$$[S_j^a, S_k^b] = i \delta_{jk} \epsilon^{abc} S_j^c, \quad (2b)$$

which satisfy the periodic boundary conditions on the spin operators, *i.e.*,  $S_{j+L}^a \equiv S_j^a$  for  $a = x, y, z$ . Later on, we will also consider boundary conditions with discrete internal symmetry twists.

While the Hamiltonian (2) has continuous  $SO(3)$  spin-rotation symmetry, we will focus on the Abelian subgroup  $\mathbb{Z}_2^x \times \mathbb{Z}_2^z \subset SO(3)$  generated by the  $\pi$ -rotations around  $x$  and  $z$  axes. The elements of this subgroup are then represented by the unitary operators

$$R_a = \prod_{j=1}^L e^{i\pi S_j^a} = \prod_{j=1}^L i\sigma_j^a, \quad (3)$$

where  $\sigma_j^a$  are the Pauli matrices with  $a = x, y, z$ .

In addition to these internal symmetries, the Hamiltonian (2) has the translation symmetry implemented by the unitary operator  $T : S_j^a \mapsto S_{j+1}^a$ , which generates the group  $\mathbb{Z}_L$ . As we shall see, these subsymmetries capture the most important universal features of the low-energy excitations.

Phase	$\mathbb{Z}_2^x$	$\mathbb{Z}_2^y$	$\mathbb{Z}_2^z$	$\mathbb{Z}_L$	GS degeneracy
Néel <sub>x</sub>	✓	×	×	×	2
Néel <sub>y</sub>	×	✓	×	×	2
Néel <sub>z</sub>	×	×	✓	×	2
Dimer	✓	✓	✓	×	2

TABLE I: Spontaneous symmetry breaking patterns in the four gapped phases, where each checkmark indicates that the symmetry is unbroken.

Because each translation unit cell hosts a half-odd-integer spin, the Lieb-Schultz-Mattis (LSM) theorem [82, 83] and its extensions [84–86] preclude a non-degenerate gapped ground state that is simultaneously invariant under  $\mathbb{Z}_2^x \times \mathbb{Z}_2^z \times \mathbb{Z}_L$  symmetry. In the language of field theory, this ingapability condition can be thought of resulting from a mixed anomaly between  $\mathbb{Z}_L$  translation symmetry and the internal  $\mathbb{Z}_2^x \times \mathbb{Z}_2^z$  symmetry [1, 78, 87–89], which we refer to as the LSM anomaly.

### B. Adjacent gapped phases

Consistently with the LSM anomaly, Hamiltonian (2) has gapless spectrum. Its low-energy properties are described by the  $SU(2)_1$  Wess-Zumino-Witten (WZW) conformal field theory (CFT), *i.e.*, the compact boson CFT with central charge  $c = 1$  at the self-dual radius  $R = \sqrt{2}$  [90, 91]. The Hamiltonian density for this CFT is

$$\mathcal{H} = \frac{v}{2} \left[ \frac{1}{K} (\partial_x \theta)^2 + K (\partial_x \phi)^2 \right] \quad (4)$$

where  $\theta$  and  $\phi$  are dual compact boson fields with  $\theta \sim \theta + \sqrt{2\pi}$ ,  $\phi \sim \phi + \sqrt{2\pi}$ , and the coupling  $K = 1$ .

Because of the underlying LSM anomaly, any gapped phase stabilized by symmetric deformations breaks  $\mathbb{Z}_2^x \times \mathbb{Z}_2^z$  internal or  $\mathbb{Z}_L$  translation symmetries spontaneously, see Table I. There are four such adjacent gapped symmetry-breaking phases [80, 92–94], as shown in Fig. 1.

*a. Dimer phase.* Tuning up the antiferromagnetic next-nearest-neighbor exchange term

$$\Delta H = J \sum_{j=1}^L \mathbf{S}_j \cdot \mathbf{S}_{j+2}, \quad J > 0 \quad (5)$$

generates at low-energy limit the perturbation

$$\delta \mathcal{H} \sim \lambda_\phi \cos(\sqrt{8\pi} \phi(x)), \quad \lambda_\phi < 0, \quad (6)$$

with scaling dimension  $\Delta = 2/K$ , which is marginal when  $K = 1$ . The field theory for the spin-1/2 Heisenberg chain can also be written as

$$S = S_{\text{WZW}} + \lambda \int dx d\tau \mathbf{J}_L \cdot \mathbf{J}_R \quad (7)$$

$S_{\text{WZW}}$  is the WZW model action for the  $\text{SU}(2)_1$  CFT. There is a critical coupling  $J_c \sim 0.2411$ , and both  $\lambda_\phi$  and  $\lambda$  are proportional to  $J - J_c$ . When  $J > J_c$  ( $J < J_c$ ),  $\lambda$  is marginally relevant (irrelevant). Since  $\lambda$  is the only term that breaks the  $\text{SO}(4)$  symmetry of the WZW theory, at the critical coupling  $J = J_c$ , the system is tuned to the point where the  $\text{SO}(4)$  symmetry emerges even at short distance, as the leading  $\text{SO}(4)$  breaking term is tuned to zero, and the other terms breaking the  $\text{SO}(4)$  symmetry are irrelevant.

The  $\text{SO}(4)$  symmetry of Eq. 7 with  $\lambda = 0$  will become manifest in the ED data to be discussed in the next few sections. In fact the model has an even larger  $\text{O}(4)$  symmetry, whose improper  $Z_2$  rotation corresponds to the reflection of the chain. In field theory this improper  $Z_2$  exchanges  $\text{SU}(2)_L$  and  $\text{SU}(2)_R$ . Since it is not clear how to insert a flux of reflection, the improper  $Z_2$  will not be discussed on the equal footing as the rest of the symmetry.

When  $J > J_c$ , the perturbation (6) opens a gap in the spectrum and pins the value of the field  $\phi$  to the values  $\phi = 0, \sqrt{2\pi}/2$ . There are two degenerate ground states that are distinguished by the non-vanishing expectation value of the dimer order parameter

$$m_d = \frac{1}{L} \sum_{j=1}^L (-1)^j \mathbf{S}_j \cdot \mathbf{S}_{j+1}. \quad (8)$$

This order parameter preserves the internal  $\mathbb{Z}_2^x \times \mathbb{Z}_2^z$  symmetry while breaking the  $\mathbb{Z}_L$  translation symmetry by one lattice site.

*b. Néel phases.* The remaining three gapped phases are stabilized by the easy-axis anisotropy couplings

$$\Delta H_a = \Delta_a \sum_{j=1}^L (S_j^a S_{j+1}^a + J S_j^a S_{j+2}^a), \quad (9)$$

with  $a = x, y, z$ , which preserve the  $\mathbb{Z}_2^x \times \mathbb{Z}_2^z \times \mathbb{Z}_L$  symmetry while breaking the  $\text{SO}(3)$  spin-rotation symmetry down to a  $\text{U}(1)_a$  symmetry along  $a$ -axis. For  $\Delta_a > 0$ , these perturbations open a gap in the spectrum with twofold degenerate ground states that are distinguished by the non-vanishing expectation value of the order parameters

$$m_a = \frac{1}{L} \sum_{j=1}^L (-1)^j S_j^a, \quad (10)$$

which preserves the  $\mathbb{Z}_2^a$  while breaking both  $\mathbb{Z}_2^b$  ( $b \neq a$ ) and  $\mathbb{Z}_L$  symmetries spontaneously. Importantly, the composition  $R_b T$  of the spontaneously broken spin-flip operators  $R_b$  and translation  $T$  symmetries is also preserved.

At low-energy limit, the anisotropy terms (9) have different effects for  $a = x, y, z$ <sup>1</sup>. When  $\Delta_z > 0$ , the term

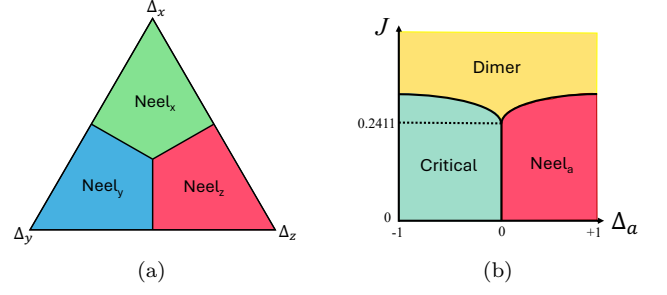


FIG. 1: Two-dimensional slices of the phase diagram of antiferromagnetic Heisenberg chain (2) perturbed by the deformations (5) and (9). (a) Three Néel phases at the slice  $J = 0$  and  $\sum_a \Delta_a \leq 1$ , with  $0 \leq \Delta_a$  and the center of the triangle being the point  $\Delta_a = 0$ . (b) Dimer and Néel<sub>a</sub> phases at the two-dimensional slice with  $J, \Delta_a \neq 0$ .

(9) renormalizes the parameter  $K$  to  $K' \approx K + c \Delta_z$  with positive constant  $c$  and leads to the perturbation

$$\delta \mathcal{H} \sim g_a \cos(\sqrt{8\pi} \phi(x)), \quad g_a > 0, \quad (11)$$

which is now relevant with scaling dimension  $\Delta = 2/K' < 2$ . This term opens a gap by pinning the field  $\phi$  to the values  $\phi = \sqrt{2\pi}/4, 3\sqrt{2\pi}/4$ , which describes the Néel<sub>z</sub> phase.

When  $\Delta_b > 0$  ( $b = x, y$ ), the term (9) renormalizes the parameter  $K$  to  $K' \approx K - c \Delta_b$  with a positive constant  $c$  and leads to the relevant perturbation

$$\delta \mathcal{H} \sim g_b \cos(\sqrt{8\pi} \theta(x)), \quad (12)$$

with scaling dimension  $\Delta = 2K' < 2$ . The coupling  $g_b < 0$  ( $g_b > 0$ ) when  $b = x$  ( $b = y$ ), and, hence, the dual field  $\theta$  is pinned to the values  $\theta = 0, \sqrt{2\pi}/2$  ( $\theta = \sqrt{2\pi}/4, 3\sqrt{2\pi}/4$ ) which describes the Néel<sub>x</sub> (Néel<sub>y</sub>) phase.

### III. LOW-ENERGY EXCITATIONS FROM EXACT DIAGONALIZATION

We aim to match the low-energy excitations of spin- $\frac{1}{2}$  antiferromagnetic Heisenberg chain with the anyon content of an appropriate symTO. To do so, we are going to perform exact diagonalization (ED) with  $\mathbb{Z}_2^x \times \mathbb{Z}_2^z$  symmetry twisted boundary conditions for different system sizes (even and odd  $L$ ). This allows one to organize the low-energy excitations in terms of irreducible representations (irreps) of appropriate global (emergent or emanant) symmetries in distinct flux sectors. For exact lattice symmetries, such irreps consist of exactly degenerate states, while for emergent symmetries they would be approximately degenerate.

Because of the LSM anomaly in the  $\mathbb{Z}_2^x \times \mathbb{Z}_2^z \times \mathbb{Z}_L$  symmetry, the possible multiplet structure of the low-energy irreps is already constrained. More precisely, first

<sup>1</sup> Here we follow the convention of Ref. 94 when identifying perturbations (9) at the lattice level with their continuum counterparts.



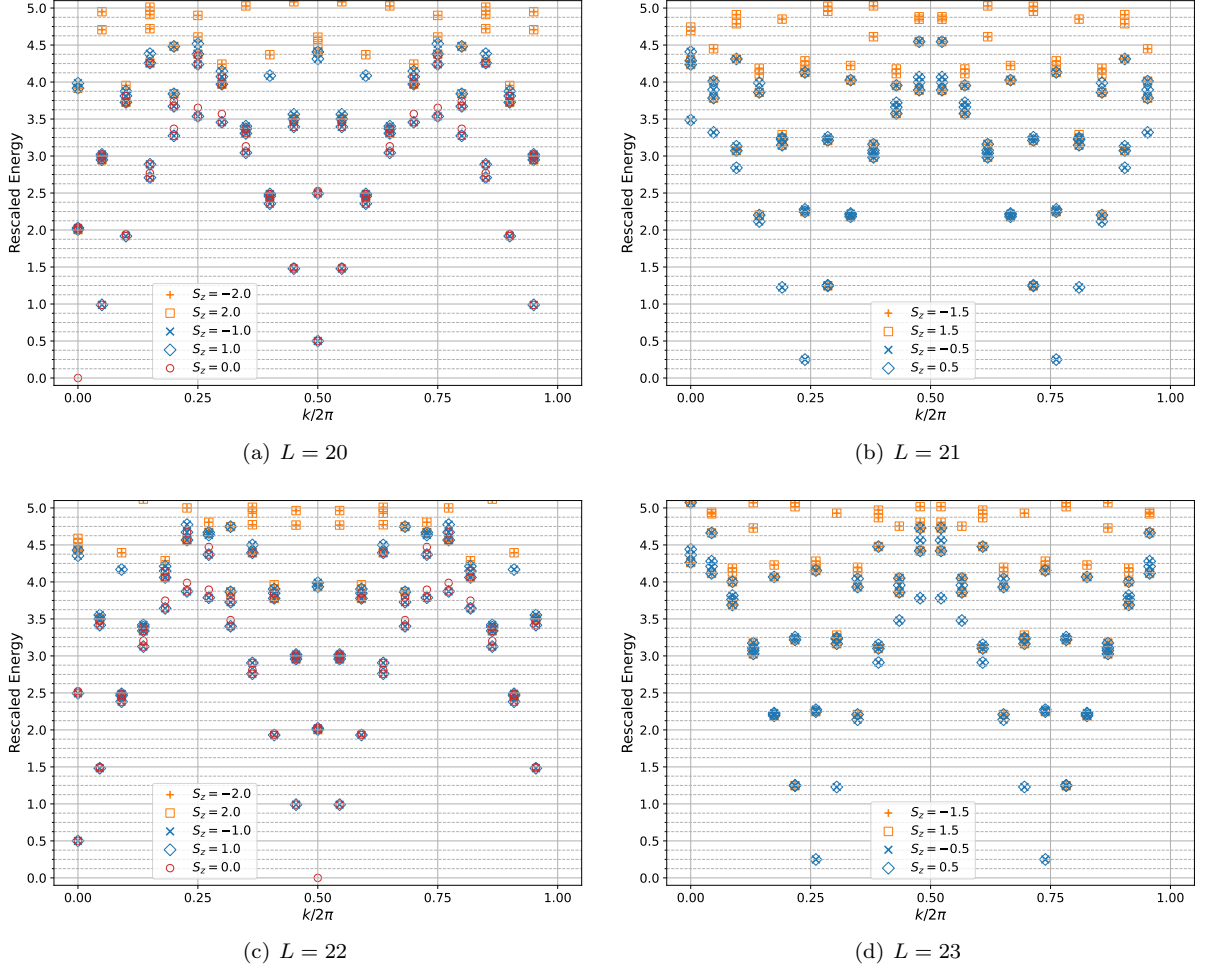


FIG. 2: ED spectra for the Heisenberg model with PBC for  $L = 20, 21, 22, 23$ . The momentum is normalized by  $2\pi$ . The full lattice symmetry is  $SO(3) \times \mathbb{Z}_L$ . But as we noted the lattice model at  $J = J_c$  has good emergent  $SO(4)$  symmetry even at relatively short distance, and this  $SO(4)$  symmetry leads to the nearly fourfold degeneracy for some of the low-energy states.

we note that the internal symmetry group  $\mathbb{Z}_2^x \times \mathbb{Z}_2^z$  obeys the (projective) algebra

$$R_x R_z = (-1)^L R_z R_x. \quad (13)$$

The dependence on the number of sites  $L$  means that the internal symmetry group is represented by non-trivial projective representation when  $L$  is odd. In this case, every eigenstate is at least doubly degenerate, *i.e.*, the entire spectrum can be organized into two-dimensional projective irreps of the  $\mathbb{Z}_2^x \times \mathbb{Z}_2^z$ . Similarly, imposing  $\mathbb{Z}_2^a$ -twisted boundary conditions by inserting a symmetry defect between sites  $L$  and  $1$  modifies the translation operator as

$$T_a = e^{i\pi S_1^a} T, \quad (14a)$$

which now satisfies the algebra

$$T_a^L = R_a, \quad T_a R_b = -R_b T_a, \quad b \neq a. \quad (14b)$$

This means that (i) the global symmetry group is now changed to  $\mathbb{Z}_2^b \times \mathbb{Z}_{2L}^a$  and (ii) this group is represented projectively.

As we discussed previously, an  $O(4)$  symmetry already emerges at short distance in the Hamiltonian we simulate. The  $O(4)$  symmetry also manifests in the ED spectrum: some of the low energy states constitute nearly degenerate quadruple states, as they form a vector representation of the  $SO(4)$ . The extra improper  $\mathbb{Z}_2$  rotation (reflection) of  $O(4)$  ensures the degeneracy between states with momentum  $k$  and  $-k$ . We have also verified that a perturbation in the Hamiltonian that breaks reflection will lift the degeneracy between  $k$  and  $-k$ , but keeps the degeneracy of the quadruple states. See Fig. 3 for the ED spectra.

We note that under any boundary condition, translation by two sites,  $j \mapsto j + 2$  commutes with all internal symmetries. As we shall see, on the low-energy degrees of freedom the translation by two sites will flow to

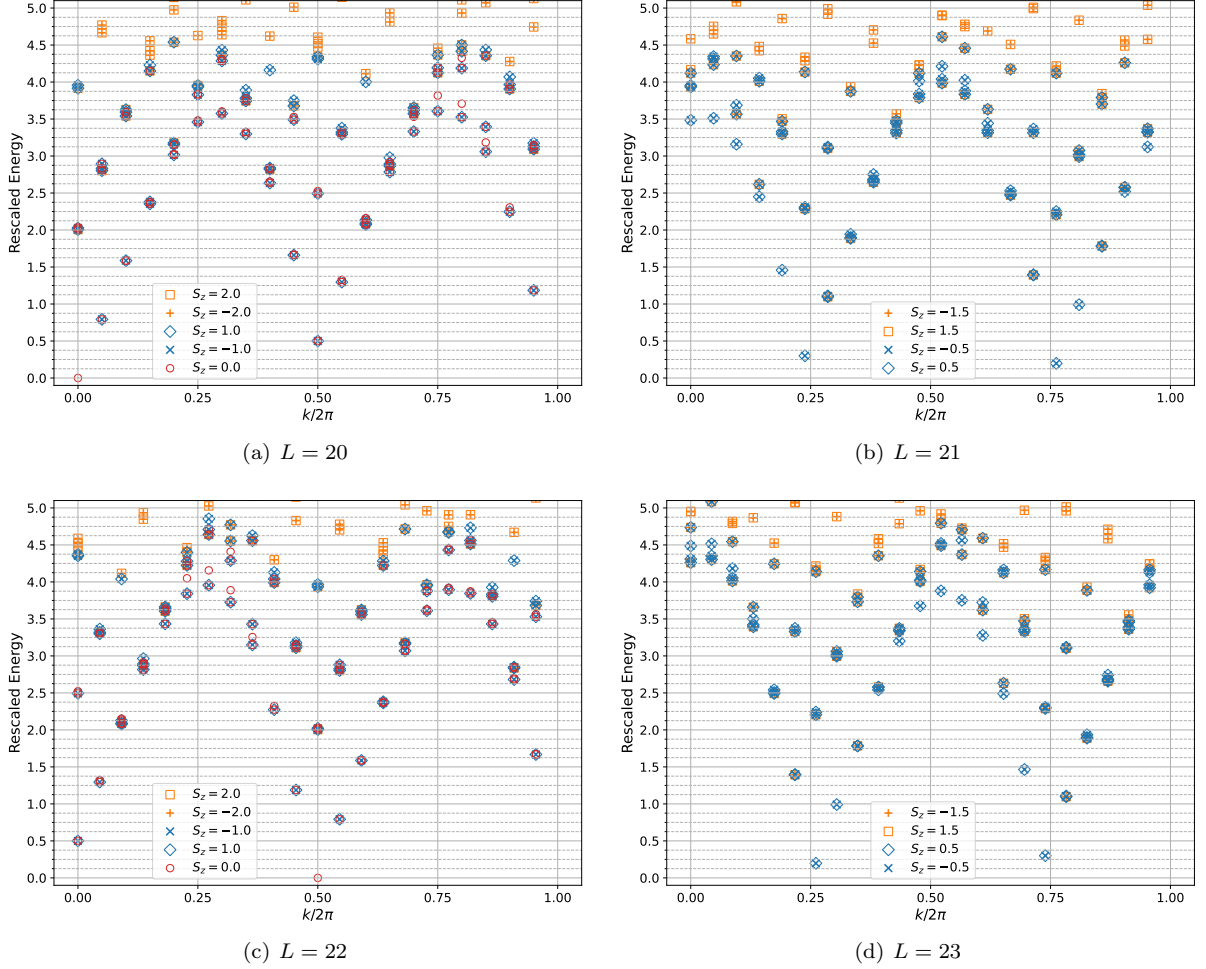


FIG. 3: ED spectra for the Heisenberg model under PBC with a chiral perturbation for  $L = 20, 21, 22, 23$ . The chiral perturbation term is  $0.1 \sum_j \mathbf{S}_j \cdot (\mathbf{S}_{j+1} \times \mathbf{S}_{j+2})$ . The degeneracy of states labeled by  $(k, S_z^{\text{tot}})$  is preserved. However, as the improper  $\mathbb{Z}_2$  reflection symmetry is broken, 6-fold degeneracy of states with momentum  $k$  and  $-k$  is lifted.

pure continuum translation symmetry while there will be an exact  $\mathbb{Z}_2^t$  symmetry that emanate from translation by one site [1, 95]. Coseting by translation by two sites, we are going to identify the low-energy emanant symmetry group as  $\mathbb{Z}_2^x \times \mathbb{Z}_2^z \times \mathbb{Z}_2^t$ .

#### A. The spectrum calculation

With the above understanding, we perform ED and organize the spectrum into the irreps of  $\mathbb{Z}_2^x \times \mathbb{Z}_2^z \times \mathbb{Z}_2^t$  symmetry. More specifically, we diagonalize the Hamiltonian

$$H = \sum_{j=1}^L \mathbf{S}_j \cdot \mathbf{S}_{j+1} + J \sum_{j=1}^L \mathbf{S}_j \cdot \mathbf{S}_{j+2}, \quad (15)$$

with the coupling  $J$  tuned to the value  $J = 0.2411$ . While the low-energy properties are described by the same CFT for  $0 \leq J \leq J_c$ , this particular choice tunes the lattice

model to the multicritical point at the intersection of four gapped phases described in Sec. II B and makes the ED spectrum closer to the tower of excitations in the CFT.

To cover all the flux sectors of  $\mathbb{Z}_2^x \times \mathbb{Z}_2^z$  symmetry we are going to impose either periodic boundary conditions (PBC)

$$S_{j+L}^a \equiv S_j^a, \quad (16a)$$

or  $\mathbb{Z}_2^z$ -twisted boundary conditions (TBC)

$$S_{j+L}^a \equiv R_z S_j^a R_z^\dagger. \quad (16b)$$

Without loss of generality, we only consider the boundary conditions twisted by  $\mathbb{Z}_2^z$  symmetry since the remaining non-trivial twists by elements in  $\mathbb{Z}_2^x \times \mathbb{Z}_2^z$  amounts to a permutation of labels due to the spin rotation symmetry of Hamiltonian (15). Under PBC, the momentum  $k$  is defined by

$$T|\psi_k\rangle = e^{ik}|\psi_k\rangle, \quad (17)$$

with  $k = 2\pi n/L$  and  $n = 0, 1, \dots, L-1$ . For TBC, the appropriate quantum number  $k$  is the eigenphase of the twisted translation  $T_z$ ,

$$T_z|\psi_k\rangle \equiv e^{i\pi S_1^z} T|\psi_k\rangle = e^{ik}|\psi_k\rangle, \quad (18)$$

with  $k = 2\pi n/2L$  and  $n = 0, 1, \dots, 2L-1$ . which commutes with the  $\mathbb{Z}_2^z$ -twisted Hamiltonian.

The low-energy spectra of Hamiltonian (15) is periodic in  $L$  modulo 4, see Fig. 2. For both PBC and TBC, we compute the spectra for chains with  $L = 20, 21, 22, 23$ , thereby sampling every congruence class  $L \equiv 0, 1, 2, 3 \pmod{4}$ . We are going to further interpret the case of odd  $L$  as the insertion of emanant  $\mathbb{Z}_2^t$  symmetry flux relative to the case of even  $L$  [1, 96, 97]. Hence, by performing ED with these four system sizes  $L$  together with both PBC and TBC we are going to organize the spectra of Hamiltonian (15) in terms of the irreps in every possible flux sector of emanant  $\mathbb{Z}_2^x \times \mathbb{Z}_2^z \times \mathbb{Z}_2^t$  symmetry.

We also normalize the energy  $E$  of each eigenstate to that of their conformal weight using the CFT spectrum

$$E(L) = \epsilon L + \frac{2\pi v}{L} \left[ (h + \bar{h} + N + \bar{N}) - \frac{c}{12} \right] + O(1/L^2), \quad (19)$$

where  $\epsilon$  gives the energy density,  $v$  denotes spinon velocity, and  $c = 1$  for the  $SU(2)_1$  WZW theory. The terms  $(h + \bar{h})$  and  $(N + \bar{N})$  give the conformal weights of the corresponding primaries and descendants, respectively. For even  $L$  under PBC, the ground state has total conformal weight  $h + \bar{h} = N + \bar{N} = 0$ . Then using the groundstate energies at  $L = 20, 22, 24$ , we obtain through fitting

$$\epsilon = -0.401954 \pm 0.000000, \quad (20a)$$

$$v = 1.176693 \pm 0.000131. \quad (20b)$$

These are bulk quantities and therefore apply to all boundary conditions. Subtracting the extensive term and rescaling by  $2\pi v/L$  yields energy in units of conformal weights deliver

$$\tilde{E}(L) \equiv \frac{L}{2\pi v} [E(L) - \epsilon L] + \frac{c}{12} = h + \bar{h} + N + \bar{N}, \quad (21)$$

which we use in all plots of ED spectra.

## B. The spectra for PBC

The energy spectrum on a lattice is organized by the lattice symmetry. For a lattice with  $L$  and PBC, the lattice symmetry group is  $\mathbb{Z}_2^x \times \mathbb{Z}_2^z \times \mathbb{Z}_L^t$ , generated by the pairwise commuting operators  $R_x$ ,  $R_z$ , and  $T$ . In contrast, for a lattice with odd  $L$  and PBC, the lattice symmetry group is  $(\mathbb{Z}_2^x \times_\omega \mathbb{Z}_2^z) \times \mathbb{Z}_L^t$ , generated by the operators  $R_x$ ,  $R_z$ , and  $T$ . Here, by subscript  $\omega$  we denote the 2-cocycle in the group cohomology class  $[\omega] \in H^2(\mathbb{Z}_2^x \times \mathbb{Z}_2^z, \mathbb{R}/\mathbb{Z}) \cong \mathbb{Z}_2$  that specifies the nontrivial global projective representation of  $\mathbb{Z}_2^x \times \mathbb{Z}_2^z$  due to the

anticommutation  $R_x R_z = -R_z R_x$ <sup>2</sup>.

Since the  $\mathbb{Z}_L^t$  translation symmetry commutes with the Hamiltonian, the momentum  $k \pmod{2\pi}$  is a good quantum number. From the ED calculations, we observe that for even  $L$ , the low-energy excitations belong to two branches centered around momentum sectors at  $k = 0, \pi$  (see Fig. 2). The ground state is a non-degenerate singlet with  $S_z^{\text{tot}} = 0$ . Its momentum is  $k = 0$  for  $L = 0 \pmod{4}$  and  $k = \pi$  for  $L = 2 \pmod{4}$ . On even- $L$  chains, the translation  $T$  and spin-flip operators  $R_x$ ,  $R_z$  all commute with one another, so every eigenstate can be simultaneously labeled by the triplet  $(R_x, R_z, e^{ik})$ .

For odd  $L$ , the low-energy excitations belong to two momentum sectors at  $k = \pi/2$  and  $3\pi/2$  (see Fig. 2). Finite-size quantization of picking  $k \in \{2\pi n/L | n \in \mathbb{Z}_L\}$  shifts groundstate momenta slightly off  $\pi/2$  and  $3\pi/2$  in the spectra, which converge back to these values in the  $L \rightarrow \infty$  limit. In this case, the two spin-flip operators anticommute ( $R_x R_z = -R_z R_x$ ) while both still commuting with translations  $T$ . This forces every energy level in a given momentum sector to be at least twofold degenerate, *i.e.*, each momentum sector consists of two-dimensional (2D) projective irreps of  $\mathbb{Z}_2^x \times_\omega \mathbb{Z}_2^z$ . In particular, the groundstate subspace is fourfold degenerate and realizes two copies of such 2D projective irreps that carry spin- $1/2$ , *i.e.*,  $S_z^{\text{tot}} = \pm 1/2$ . In the groundstate subspace, we can express the symmetry operators  $R_x$ ,  $R_z$ , and  $T$  as  $4 \times 4$  matrices. We choose a basis in which  $T$  remains diagonal and express the remaining symmetry operators  $R_x$  and  $R_z$  as  $2 \times 2$  matrices in each momentum eigensector, see Table II.

We note that low-energy sectors carry crystal momenta that always differ by multiple of  $\pi$ . Thus the translation symmetry in the continuum limit is generated by two-site translation  $T^2$ . The one-site translation  $T$ , or more precisely  $T/\sqrt{T^2}$ , becomes a  $\mathbb{Z}_2^t$  internal symmetry in the continuum limit. The different lattice size for PBC can then be viewed as different symmetry twists of  $\mathbb{Z}_2^t$  internal symmetry emanating from the translation symmetry. The fact that a different  $\mathbb{Z}_2^t$  twist also shifts the low-energy momenta by  $k \approx \pm\pi/2$  is a signature of the fact that the  $\mathbb{Z}_2^t$  symmetry in the continuum is anomalous [98].

Since the rescaled energies are in units of conformal weights, the spectra show the existence of  $SU(2)_1$  WZW CFT's two Virasoro primaries in the untwisted sector [99]. The identity **1** with  $(h, \bar{h}) = (0, 0)$  appear as the unique even- $L$  ground state, and the spinon doublet  $g^{\alpha\beta}$  with  $(h, \bar{h}) = (\frac{1}{4}, \frac{1}{4})$  appear as the first excited states in even- $L$  spectra. Furthermore, we are going to interpret the deviation of the ground-state momenta from  $\pi/2$  and  $3\pi/2$  as the topological spin of these excitations. These spins can be fractional – see the discussion in Section IV.

<sup>2</sup> From now on, we use  $\times_\omega$  to denote nontrivial projective algebra between generators of two subgroups.

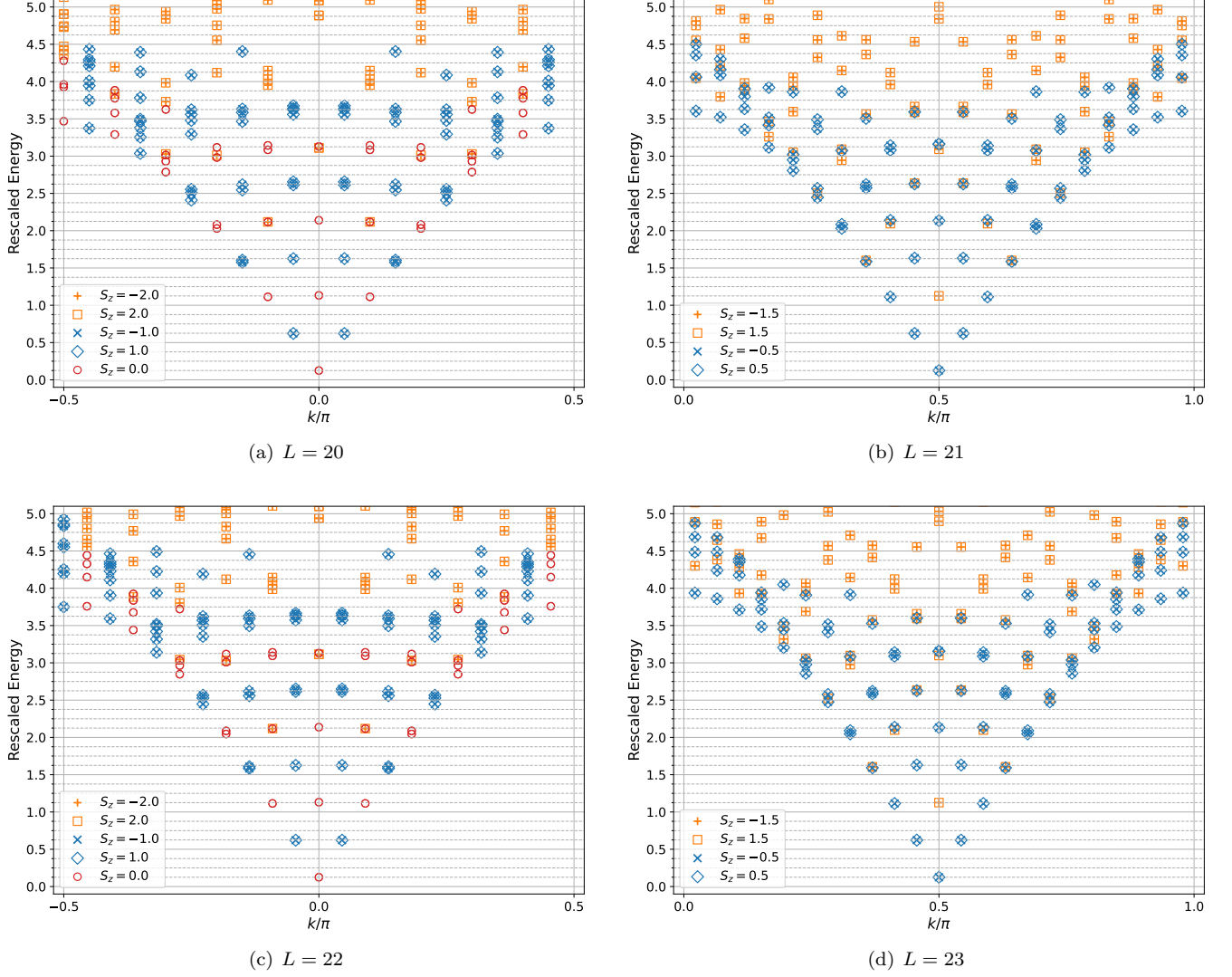


FIG. 4: ED spectra for the Heisenberg model with  $\mathbb{Z}_2^z$ -twisted boundary conditions for  $L = 20, 21, 22, 23$ . The momentum is normalized by  $\pi$ . The full lattice symmetry is  $\frac{U(1)_z \times \mathbb{Z}_{2L}^z}{\mathbb{Z}_2^z} \rtimes \mathbb{Z}_2^x$ .

### C. The spectra for TBC

Under the  $\mathbb{Z}_2^z$ -twisted boundary conditions for both  $L$  even and odd, the twisted translation operator  $T_z = e^{i\pi S_z^1} T$  anticommutes with the internal spin-flip symmetry generator  $R_x$ , *i.e.*,  $R_x T_z = -T_z R_x$  and satisfy  $T_z^L = R_z$ ,  $T_z^{2L} = 1$ . Thus, the lattice symmetry group is  $(\mathbb{Z}_2^x \times_\omega \mathbb{Z}_{2L}^z)$ , generated by  $R_x$  and  $T_z$ . Because of this projective algebra, one cannot simultaneously diagonalize twisted translation and internal spin-flip symmetries. Instead, we consider eigenvalues of the two-site twisted translation  $T_z^2$ , which commutes with the internal spin-flip generator  $R_x$ . We therefore work in a reduced Brillouin zone, identifying  $k \equiv k + \pi$  (see Fig. III), and treat the one-site twisted translation  $T_z$  as the emanant internal symmetry  $\mathbb{Z}_2^t$ .

For even  $L$ , only the twisted-momentum sector  $k = 0 \bmod \pi$  appears.  $R_z$  commutes with both  $R_x$  and  $T_z$ , so eigenstates carry well-defined eigenvalues  $(R_z, e^{ik})$ . However, the projective algebra  $T_z R_x = -R_x T_z$  forces every eigenenergy sector to be at least twofold degenerate. The groundstates are twofold degenerate, each with  $S_z^{\text{tot}} = 0$ . The first excited level has four degenerate eigenstates which split into two distinct momenta, each of which are doubly degenerate with  $S_z^{\text{tot}} = \pm 1$ .

For odd  $L$ , only the momentum sector  $k = \pi/2 \bmod \pi$  appears.  $R_z$  commutes with  $T_z$  and both  $R_z$  and  $T_z$  anticommute with  $R_x$ . Thus, each level is twofold degenerate in both  $R_x$  and  $R_z$ , with  $T_z$  and  $R_z$  flipping the  $R_x$ -eigenvalues and  $R_x$  flipping the  $R_z$ -eigenvalues. Note that because we identify  $k \equiv k + \pi$ ,  $e^{ik} \equiv -e^{ik}$ . The twisted translation  $T_z$  defines a consistent momentum despite its anticommutation relations with spin-flip



$L \bmod 4$	Degeneracy	$e^{ik}$	$R_x$	$R_y$	$R_z$	$S_z^{\text{tot}}$
0	1	1	+1	+1	+1	0
1	2	i	$\begin{pmatrix} 0 & i \\ i & 0 \end{pmatrix}$	$\begin{pmatrix} 0 & 1 \\ -1 & 0 \end{pmatrix}$	$\begin{pmatrix} i & 0 \\ 0 & -i \end{pmatrix}$	$\begin{pmatrix} \frac{1}{2} & 0 \\ 0 & -\frac{1}{2} \end{pmatrix}$
	2	-i	$\begin{pmatrix} 0 & i \\ i & 0 \end{pmatrix}$	$\begin{pmatrix} 0 & 1 \\ -1 & 0 \end{pmatrix}$	$\begin{pmatrix} i & 0 \\ 0 & -i \end{pmatrix}$	$\begin{pmatrix} \frac{1}{2} & 0 \\ 0 & -\frac{1}{2} \end{pmatrix}$
2	1	-1	+1	+1	+1	0
3	2	i	$\begin{pmatrix} 0 & i \\ i & 0 \end{pmatrix}$	$\begin{pmatrix} 0 & 1 \\ -1 & 0 \end{pmatrix}$	$\begin{pmatrix} i & 0 \\ 0 & -i \end{pmatrix}$	$\begin{pmatrix} \frac{1}{2} & 0 \\ 0 & -\frac{1}{2} \end{pmatrix}$
	2	-i	$\begin{pmatrix} 0 & i \\ i & 0 \end{pmatrix}$	$\begin{pmatrix} 0 & 1 \\ -1 & 0 \end{pmatrix}$	$\begin{pmatrix} i & 0 \\ 0 & -i \end{pmatrix}$	$\begin{pmatrix} \frac{1}{2} & 0 \\ 0 & -\frac{1}{2} \end{pmatrix}$

TABLE II: Representations of symmetry operators in the groundstate subspace of Hamiltonian (15) for fixed momentum eigensectors with PBC.

symmetry generators  $R_x$  and  $R_z$ . The groundstates are twofold degenerate doublets, with  $S_z^{\text{tot}} = \pm 1/2$ . The first excited level again has four states, splitting into two distinct momenta, each of which are doubly degenerate with  $S_z^{\text{tot}} = \pm 1/2$ .

For both even and odd  $L$ , the groundstate subspace furnishes a 2D irrep of the algebra generated by  $\{R_x, R_z\}$ . More concretely, for odd  $L$ , the irrep is just realized by Pauli matrices on the doublet. For even  $L$ , only  $R_x$  and  $T_z$  form a noncommuting pair, while  $R_z$  acts trivially (proportional to identity) on the 2D groundstate subspace. The groundstate properties of the TBC spectra are summarized in Table III.

Finally, inserting a  $\mathbb{Z}_2^z$  defect selects the twisted sector of the  $c = 1$  theory [100]. Its lowest Virasoro primary has conformal weights  $(h, \bar{h}) = (\frac{1}{16}, \frac{1}{16})$ , exactly matching the rescaled energy of the ED groundstates with TBC.

#### D. Emanant symmetries and anomalies

We observe that the lattice symmetry groups depend on the system size and the boundary conditions. As we discussed, for all these symmetry groups, (twisted) translation by two-sites commutes with all other elements. It is, thus, convenient to coset the lattice symmetry by the subgroup generated by two-site translations, which reveals the emanant internal symmetry group [1] that the low-energy degrees of freedom transform under with possible anomaly. Identifying the emanant symmetry and its anomaly is important as they control and constrain the dynamics of the low-energy degrees of freedom.

For even  $L$  with PBC, the emanant symmetry group is  $\mathbb{Z}_2^x \times \mathbb{Z}_2^z \times \mathbb{Z}_2^{zt}$ , generated by commuting  $R_x, R_z, R_z T_z$ . Since the emanant symmetry group is Abelian, the spectrum is formed by 1D irreps.

For odd  $L$  with PBC, the emanant symmetry group is  $(\mathbb{Z}_2^x \times_\omega \mathbb{Z}_2^z) \times \mathbb{Z}_2^{zt}$ , generated by  $R_x, R_z, R_z T_z$  with anti-commuting  $R_x R_z = -R_z R_x$ .

For even  $L$  with TBC by  $\mathbb{Z}_2^z$ , the emanant symmetry

$L \bmod 4$	Degeneracy	$e^{ik}$	$R_x$	$R_y$	$R_z$	$S_z^{\text{tot}}$
0	2	$\begin{pmatrix} 1 & 0 \\ 0 & -1 \end{pmatrix}$	$\begin{pmatrix} 0 & 1 \\ 1 & 0 \end{pmatrix}$	$\begin{pmatrix} 0 & 1 \\ 1 & 0 \end{pmatrix}$	+1	0
1	2	$\begin{pmatrix} i & 0 \\ 0 & -i \end{pmatrix}$	$\begin{pmatrix} 0 & i \\ i & 0 \end{pmatrix}$	$\begin{pmatrix} 0 & 1 \\ -1 & 0 \end{pmatrix}$	$\begin{pmatrix} i & 0 \\ 0 & -i \end{pmatrix}$	$\begin{pmatrix} \frac{1}{2} & 0 \\ 0 & -\frac{1}{2} \end{pmatrix}$
2	2	$\begin{pmatrix} 1 & 0 \\ 0 & -1 \end{pmatrix}$	$\begin{pmatrix} 0 & 1 \\ 1 & 0 \end{pmatrix}$	$\begin{pmatrix} 0 & 1 \\ 1 & 0 \end{pmatrix}$	+1	0
3	2	$\begin{pmatrix} i & 0 \\ 0 & -i \end{pmatrix}$	$\begin{pmatrix} 0 & i \\ i & 0 \end{pmatrix}$	$\begin{pmatrix} 0 & 1 \\ -1 & 0 \end{pmatrix}$	$\begin{pmatrix} i & 0 \\ 0 & -i \end{pmatrix}$	$\begin{pmatrix} \frac{1}{2} & 0 \\ 0 & -\frac{1}{2} \end{pmatrix}$

TABLE III: Representations of symmetry operators in the groundstate subspace of Hamiltonian (15) with  $\mathbb{Z}_2^z$ -twisted boundary conditions.

group is  $\mathbb{Z}_2^z \times (\mathbb{Z}_2^x \times_\omega \mathbb{Z}_2^{zt})$ , generated by  $R_x, R_z, R_z T_z$  with anti-commuting  $R_x T_z = -T_z R_x$ .

For odd  $L$  with TBC by  $\mathbb{Z}_2^z$ , the emanant symmetry group is  $(\mathbb{Z}_2^x \times_\omega \mathbb{Z}_2^z) \times \mathbb{Z}_2^{zt}$ , generated by  $R_x, R_z, R_z T_z$ , with anti-commuting  $R_x T_z = -T_z R_x$  and  $R_x R_z = -R_z R_x$ .

All these latter three emanant symmetry groups are realized projectively, *i.e.*, only their 2D projective irreps appear in the spectrum. Each 2D projective irrep can be thought of as the 2D *linear* irrep of the corresponding non-Abelian group  $D_8$  that arises from the group extension that trivialize the nontrivial second cohomology class  $[\omega]$ .

We identify the anomaly of the emanant symmetries as follows. The emanant symmetry groups we have considered so far (for  $L$  odd or even with potential  $\mathbb{Z}_2^z$  twist) consist of various  $\mathbb{Z}_2$  subgroups. One way to detect an anomalous  $\mathbb{Z}_2$  subgroup is to insert its symmetry defect and compute the ground state eigenvalue under it. The symmetry defect of an anomalous  $\mathbb{Z}_2$  symmetry carries fractional charge under itself, leading to the symmetry operator squaring to  $-1$  in the defect sector [98]. For example, consider the subgroup  $\mathbb{Z}_2^z$ . From Table III, one notes that for  $L$  even, *i.e.*, the case with only  $\mathbb{Z}_2^z$  defect, the  $R_z$  operator acts as identity on the entire ground-state manifold. Thus, this subgroup is non-anomalous. Because of the permutation symmetry, we conclude that all  $\mathbb{Z}_2^a$  subgroups corresponding to internal spin-flip symmetries are non-anomalous.

Next, let's consider  $\mathbb{Z}_2^{zt}$ , which is always a subgroup of the emanant symmetries that we considered. Inserting a  $\mathbb{Z}_2^{zt}$  defect corresponds to the case of  $L$  odd with TBC. From Table III, one sees that while the ground states are twofold degenerate, both degenerate states still satisfy  $(R_z T_z)^2 = 1$ . In other words, the subgroup  $\mathbb{Z}_2^{zt}$  itself does not carry a self-anomaly. In the similar way one finds that the subgroups  $\mathbb{Z}_2^{xt}$  and  $\mathbb{Z}_2^{yt}$  are also anomaly free.

Finally, the diagonal subgroup  $\mathbb{Z}_2^t$  of the emanant  $\mathbb{Z}_2^x \times \mathbb{Z}_2^z \times \mathbb{Z}_2^{zt}$  symmetry is anomalous as alluded before. This is because in the presence of  $\mathbb{Z}_2^z$  twist, the ground state acquires fractional eigenvalue of  $i$  under  $\mathbb{Z}_2^t$  subgroup, see Table II for odd  $L$ . Combining the fact

that each of the subgroups  $\mathbb{Z}_2^x$ ,  $\mathbb{Z}_2^z$ , and  $\mathbb{Z}_2^{zt}$  is anomaly-free while their composition  $\mathbb{Z}_2^t$  is anomalous, we conclude that the emanant symmetry in the continuum limit is described by  $\mathbb{Z}_2^x \times \mathbb{Z}_2^z \times \mathbb{Z}_2^{zt}$  with a type-III mixed anomaly. A consequence of this is that whenever a defect of an anomaly-free  $\mathbb{Z}_2$  subgroup is inserted, the remaining subgroup acts projectively on the twisted sector, which we verified in Tables II and III.

#### IV. IDENTIFYING SYMTO $\mathcal{D}(D_8)$ FROM SECTORS OF LOW-ENERGY SPECTRA

In this section, we are going to use the low-energy spectra computed in Sec. III to compute the symTO of the gapless Heisenberg model, which as we shall turn out to be the quantum double  $\mathcal{D}(D_8)$  of the dihedral group  $D_8$ .

We obtain the symTO matching the low-energy properties, by organizing the spectra into the degenerate low-energy sectors each which are labeled by an bulk anyon of the symTO. To do so, we need to extract the following data: the total number  $N$  of anyons, the topological spin  $s$  of each anyon, and the quantum dimension  $d$  of each anyon.

- Distinct low-energy sectors are labeled by anyons and characterized by irreducible representations of the emanant symmetry group in a given symmetry-twisted boundary condition.
- For each anyon, the quantum dimension  $d$  is the dimension of the corresponding irrep of the emanant symmetry group.
- The topological spin  $s$  of an anyon is encoded in the momentum of the corresponding eigenstates. Denoting by  $k$  the crystal momentum of a set of degenerate eigenstates labeled by an anyon, we define the corresponding topological spin as

$$s = \frac{L}{2\pi}(k - k_{\text{ref}}) \pmod{1}. \quad (22)$$

Here  $k_{\text{ref}}$  is reference momentum carried by the lowest energy excitation that the anyon state is created from, *e.g.*, the momentum at which a cone of excitations are centered at. For our purposes, the reference momentum takes values  $in k_{\text{ref}} \in \{0, \frac{\pi}{4}, \frac{\pi}{2}, \frac{3\pi}{4}\}$ .

We can use any low-energy multiplet in the corresponding sector to compute  $d, s$  of an anyon (see Table IV). All those low-energy states will give rise to the same anyon data  $d, s$ .

The anyons in the symTO have more data such as the F symbols. However, as we shall see the set  $\{s_a, d_a \mid a = 1, \dots, N\}$  will be sufficient for us to identify the bulk topological order. After cataloging anyons for all distinct sectors, we may verify that their fusion ring matches with that of the quantum double  $\mathcal{D}(D_8)$ , providing a consistency check on our conjecture. In the remaining of this section, we will list all the low-energy irreps of the emanant symmetry groups for all TBCs.

Anyon data	Low-energy property
$N$	# of distinct irreps in all possible TBCs
$d$	dimension of the irrep
$s$	$s = \frac{L}{2\pi}(k - k_{\text{ref}}) \pmod{1}$

TABLE IV: The correspondence between the anyon data  $\{N, s, d\}$  and . All relevant information regarding anyon data  $\{N, s, d\}$  can be retrieved from the low-energy spectrum.

Anyon	$s$	$d$	$L \pmod{4}$	$R_x$	$R_y$	$R_z$	$e^{ik}$	irrep
$\mathbb{1}$	0	1	0 (or 2)	+1	+1	+1	+1 (or -1)	$\chi(+1, +1, +1)$
$e_x$	0	1	0 (or 2)	+1	+1	-1	+1 (or -1)	$\chi(+1, -1, -1)$
$e_y$	0	1	0 (or 2)	-1	+1	-1	+1 (or -1)	$\chi(-1, -1, -1)$
$e_z$	0	1	0 (or 2)	-1	-1	+1	+1 (or -1)	$\chi(-1, +1, +1)$
$e_t$	0	1	0 (or 2)	+1	+1	+1	-1 (or +1)	$\chi(+1, +1, -1)$
$e_{xt}$	0	1	0 (or 2)	+1	-1	-1	-1 (or +1)	$\chi(+1, -1, +1)$
$e_{yt}$	0	1	0 (or 2)	-1	+1	-1	-1 (or +1)	$\chi(-1, -1, +1)$
$e_{zt}$	0	1	0 (or 2)	-1	-1	+1	-1 (or +1)	$\chi(-1, +1, -1)$

TABLE V: Relevant data for charge anyons. The corresponding emanant symmetry group for the irreps is  $\mathbb{Z}_2^x \times \mathbb{Z}_2^z \times \mathbb{Z}_2^{zt}$ .

##### A. Charge sectors

We first analyze the pure charge sectors, which correspond to the irreps of the emanant symmetry group  $\mathbb{Z}_2^x \times \mathbb{Z}_2^z \times \mathbb{Z}_2^{zt}$  without any symmetry twist. There are in total eight 1D irreps, labeled by  $a \in \{1, x, y, z, t, xt, yt, zt\}$ . These 1D irreps can also be labeled by

$$\chi(g_x, g_z, g_{zt}), \quad g_a \in \{\pm 1\}, \quad (23)$$

where  $g_a = +1$  (-1) denotes a trivial (nontrivial) charge under the corresponding  $\mathbb{Z}_2^a$ . For each irrep one can associate the local operator that transform accordingly under the emanant symmetry groups. For instance, the 1D irreps  $x, y, z$  correspond to the spin operators  $S_j^{x,y,z}$ . Similarly, the 1D irreps  $t, xt, yt, zt$  correspond to the staggered operators  $(-1)^j, (-1)^j S_j^{x,y,z}$ .

By bulk-boundary correspondence, each 1D irrep labels a distinct charge anyon in the bulk topological order. We denote a charge anyon by  $e_a$ , where  $a \in \{x, y, z, t, xt, yt, zt\}$  labels the 1D irreps. For example,

$$\chi(-1, 1, 1) \leftrightarrow e_z, \quad \chi(1, -1, -1) \leftrightarrow e_x, \quad \chi(1, 1, -1) \leftrightarrow e_t, \quad (24)$$

and so on. For the trivial charge with  $\chi(1, 1, 1)$ , we simply denote it as  $\mathbb{1}$ .

To resolve these charge sectors, we consider the low-energy spectra for PBCs at length  $L = 0 \pmod{4}$ . Having PBCs ensures that none of the internal symmetries are twisted, and lattice size of  $L = 0 \pmod{4}$  guarantees

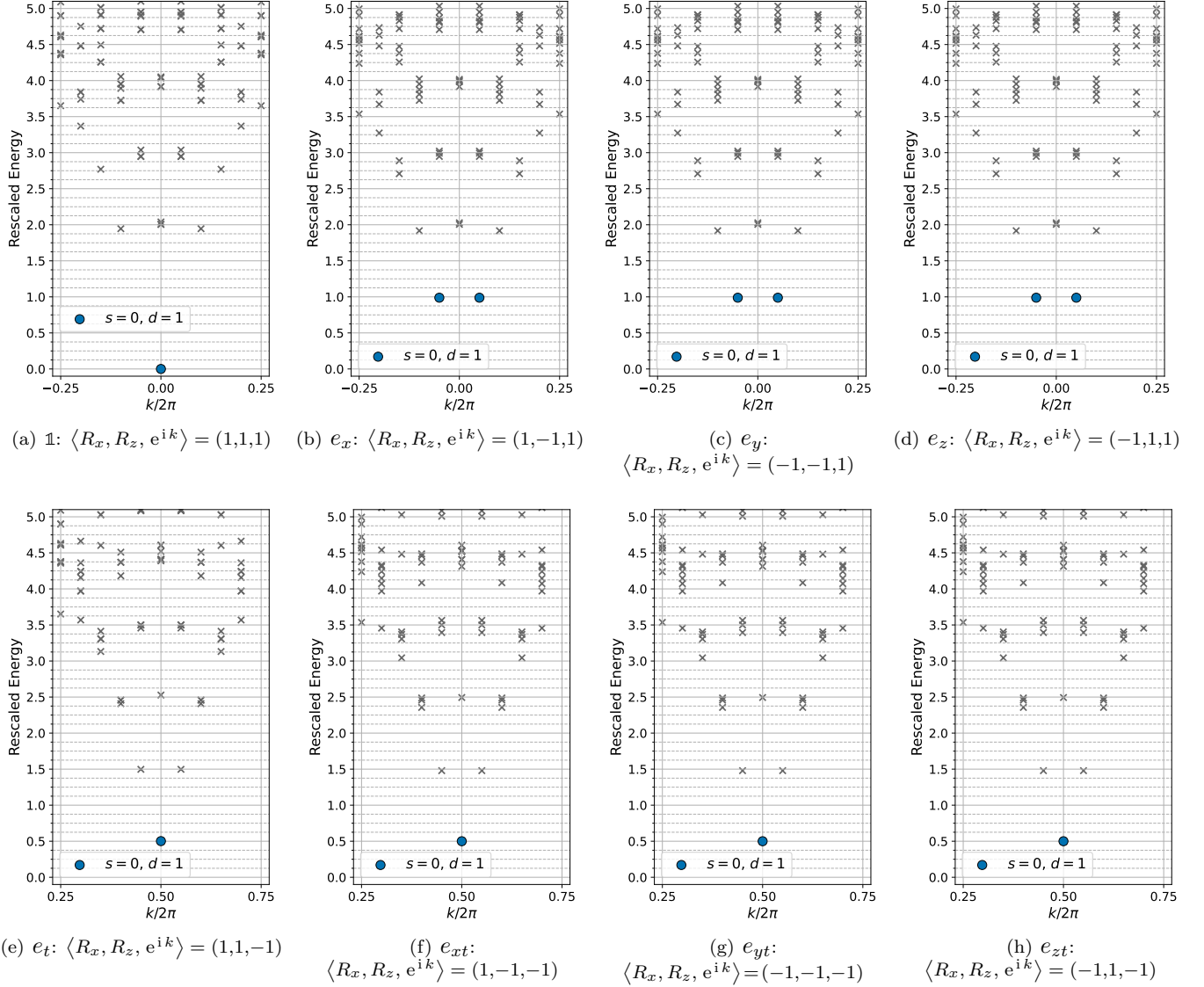


FIG. 5: Charge sector anyons, evaluated at lattice size  $L = 20$  with PBCs. Each spectrum is labeled with the anyon type and quantum numbers of the projected subspace. For the corresponding irreps, see Table V.

trivial translation flux. In principle, any even  $L$  would suffice, since translation is treated as  $\mathbb{Z}_2^t$ . In fact, in the data table for charge anyons (Table V), one finds that having  $L = 2 \pmod{4}$  simply flips the quantum number of  $e^{ik}$ , indicating the self-anomalous nature of  $\mathbb{Z}_2^t$ .

We compute the energy spectrum for  $L = 20$  with PBCs. We then project the many-body spectrum onto eight simultaneous eigensectors of  $R_x$  with eigenvalues  $\pm 1$ , of  $R_z$  with eigenvalues  $\pm 1$ , and of  $T$  with eigenvalues  $e^{ik} = \pm 1$ . The projection is possible because  $R_x$ ,  $R_z$ , and  $T$  commute for even  $L$  with PBCs. We label each subspace by the triplet  $(R_x, R_z, e^{ik})$ , which correspond to irreps  $g_x, g_z, g_{zt}$  of the group  $\mathbb{Z}_2^x \times \mathbb{Z}_2^z \times \mathbb{Z}_2^{zt}$ , respectively. In FIG. 5, we show the low-energy spectra projected into each charge sector  $L = 20$  with PBCs.

Since all irreps with PBC are 1D, all the charge anyons

have quantum dimension  $d = 1$ . Using Eq. (22), we find the topological spin for all the charge anyons to be  $s = 0$ . In the spectra, it is convenient to label the lowest energy states with the anyon label  $e_a$ . But all excitations within the same sector should be identified as the same species of anyons, though the higher-energy excitations can carry additional charges (e.g. larger momenta). The relevant data for charge anyons, including quantum numbers, irreps, and the emanant symmetry group, is summarized in Table V.

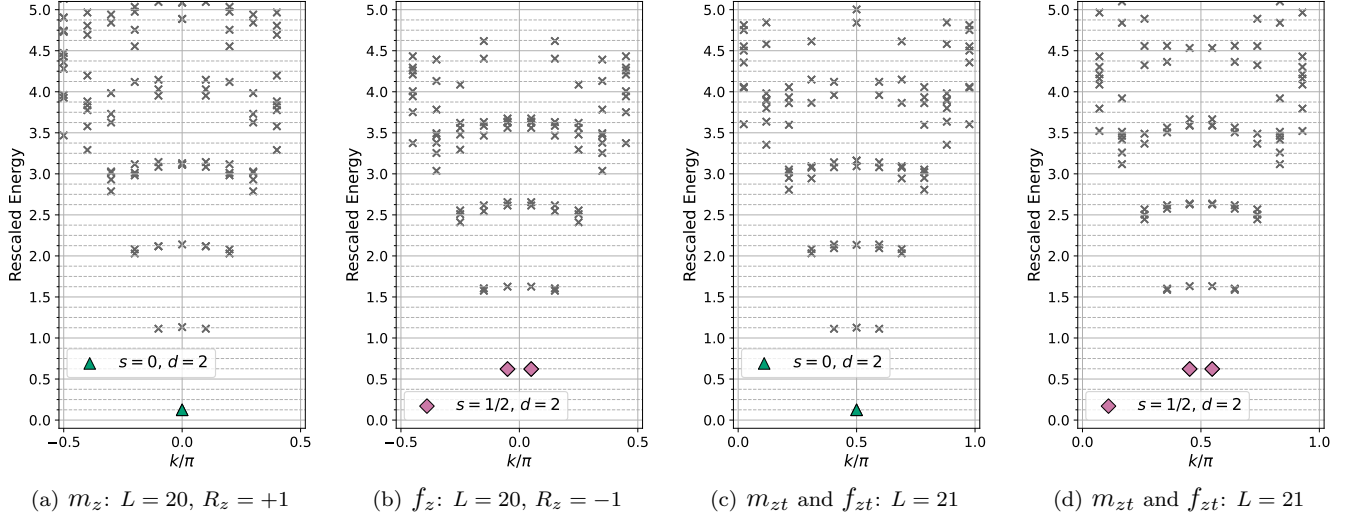


FIG. 6: (a,b) shows the low-energy sector for  $S_z$  symmetry twist and even  $L$ . Each energy level is 2-fold degenerate. (a) has  $R_z = 1$ , corresponding to anyon  $m_z$ . (b) has  $R_z = -1$ , corresponding to anyon  $f_z$ . (c,d) shows the low-energy sector for  $S_z$  symmetry twist and  $L = \text{odd}$ . Each energy level is 2-fold degenerate. The flux anyon  $m_{zt}$  are denoted by green triangles. The dyon  $f_{zt}$  are denoted by pink diamonds.

Anyon	$s$	$d$	$L \bmod 4$	BCs	$R_x$	$R_y$	$R_z$	$e^{ik}$	irrep
$m_x$	0	2	0 (or 2)	$\mathbb{Z}_2^x$ -twisted	+1	na	na	$\pm 1$	$\pi(\mathbb{Z}_2^z \times_\omega \mathbb{Z}_2^{yt})$
$m_y$	0	2	0 (or 2)	$\mathbb{Z}_2^y$ -twisted	na	+1	na	$\pm 1$	$\pi(\mathbb{Z}_2^x \times_\omega \mathbb{Z}_2^{zt})$
$m_z$	0	2	0 (or 2)	$\mathbb{Z}_2^z$ -twisted	na	na	+1	$\pm 1$	$\pi(\mathbb{Z}_2^y \times_\omega \mathbb{Z}_2^{xt})$
$m_{xt}$	0	2	1 (or 3)	$\mathbb{Z}_2^x$ -twisted	$\pm i$	na	na	$\pm i$	$\pi(\mathbb{Z}_2^z \times_\omega \mathbb{Z}_2^{yt})$
$m_{yt}$	0	2	1 (or 3)	$\mathbb{Z}_2^y$ -twisted	na	$\pm i$	na	$\pm i$	$\pi(\mathbb{Z}_2^x \times_\omega \mathbb{Z}_2^{zt})$
$m_{zt}$	0	2	1 (or 3)	$\mathbb{Z}_2^z$ -twisted	na	na	$\pm i$	$\pm i$	$\pi(\mathbb{Z}_2^y \times_\omega \mathbb{Z}_2^{xt})$

TABLE VI: Relevant data for flux anyons.

## B. Flux sectors

We now turn to flux sectors of emanant symmetry  $G_{\text{IR}} = \mathbb{Z}_2^x \times \mathbb{Z}_2^y \times \mathbb{Z}_2^{zt}$ , generated by threading symmetry fluxes around the ring (*i.e.* imposing symmetry twisted boundary conditions). Because  $G_{\text{IR}}$  has three independent  $\mathbb{Z}_2$  components, there are in total seven nontrivial pure flux sectors. Flux insertions probe projective representations and the underlying cocycle of  $G_{\text{IR}}$ , which gives rise to the type-III anomaly, playing a nontrivial role in determining the emanant symmetry groups and their irreps.

### 1. Fluxes and dyons for $\mathbb{Z}_2^z$ and $\mathbb{Z}_2^{zt}$ symmetry twists

We first focus on the cases where either one or two of the  $\mathbb{Z}_2$  components are twisted. Owing to the full  $S_3$  permutation symmetry of the spin axes, it suffices to study the subgroups  $\mathbb{Z}_2^z$  and  $\mathbb{Z}_2^{zt}$ . Note that a  $\mathbb{Z}_2^z$  twist corresponds to twisting by  $\mathbb{Z}_2^z$  for even  $L$  while a  $\mathbb{Z}_2^{zt}$  twist

corresponds to twisting by  $\mathbb{Z}_2^z$  for odd  $L$ .

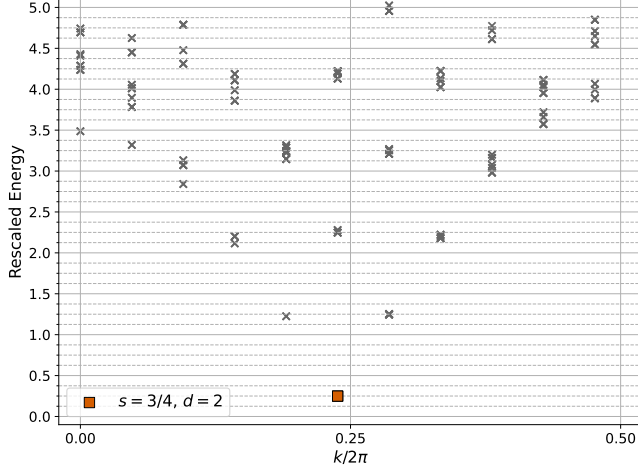
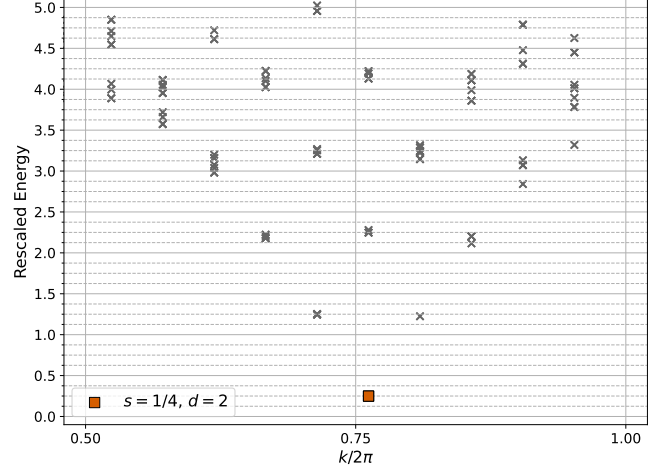
To access the flux sector of  $\mathbb{Z}_2^z$ , we compute the low-energy spectrum with  $\mathbb{Z}_2^z$ -twisted boundary conditions at lattice size  $L = 0 \pmod{4}$ . In this case, the emanant symmetry group is  $\mathbb{Z}_2^z \times (\mathbb{Z}_2^x \times_\omega \mathbb{Z}_2^{zt})$ , which has two 2-dimensional irreducible representations with  $R_z = \pm 1$ . The  $R_z = 1$  representation corresponds to a pure flux, which gives rise to the anyon  $m_z$ . The  $R_z = -1$  representation corresponds to a dyon, a bound state of  $R_z$  charge and flux, which gives rise to the anyon  $f_z$ .

Again, in principle we can also compute low-energy spectrum on lattice of size  $L = 2 \pmod{4}$ . The resulting anyons are the same, except some of the corresponding quantum numbers may be flipped (as shown in Table VI).

To access the flux sector of  $\mathbb{Z}_2^{zt}$ , we compute the low-energy spectrum with  $\mathbb{Z}_2^{zt}$ -twisted boundary conditions at lattice size  $L = 1 \pmod{4}$ . In this case, the emanant symmetry group is  $\mathbb{Z}_2^{zt} \times (\mathbb{Z}_2^x \times_\omega \mathbb{Z}_2^y)$ , which has two 2-dimensional irreducible representations with  $R_z T_z = \pm i$ . The  $R_z T_z = i$  representation corresponds to a pure flux, which gives rise to the anyon  $m_{zt}$ . The  $R_z T_z = -i$  rep-

Anyon	$s$	$d$	$L \bmod 4$	BCs	$R_x$	$R_y$	$R_z$	$e^{ik}$	irrep
$f_x$	$\frac{1}{2}$	2	0 (or 2)	$\mathbb{Z}_2^x$ -twisted	-1	na	na	$\pm 1$	$\pi(\mathbb{Z}_2^z \times_\omega \mathbb{Z}_2^{yt})$
$f_y$	$\frac{1}{2}$	2	0 (or 2)	$\mathbb{Z}_2^y$ -twisted	na	-1	na	$\pm 1$	$\pi(\mathbb{Z}_2^x \times_\omega \mathbb{Z}_2^{zt})$
$f_z$	$\frac{1}{2}$	2	0 (or 2)	$\mathbb{Z}_2^z$ -twisted	na	na	-1	$\pm 1$	$\pi(\mathbb{Z}_2^y \times_\omega \mathbb{Z}_2^{xt})$
$f_{xt}$	$\frac{1}{2}$	2	1 (or 3)	$\mathbb{Z}_2^x$ -twisted	$\pm i$	na	na	$\pm i$	$\pi(\mathbb{Z}_2^z \times_\omega \mathbb{Z}_2^{yt})$
$f_{yt}$	$\frac{1}{2}$	2	1 (or 3)	$\mathbb{Z}_2^y$ -twisted	na	$\pm i$	na	$\pm i$	$\pi(\mathbb{Z}_2^x \times_\omega \mathbb{Z}_2^{zt})$
$f_{zt}$	$\frac{1}{2}$	2	1 (or 3)	$\mathbb{Z}_2^z$ -twisted	na	na	$\pm i$	$\pm i$	$\pi(\mathbb{Z}_2^y \times_\omega \mathbb{Z}_2^{xt})$

TABLE VII: Relevant data for dyons.

(a)  $s_t$ :  $L = 21$ (b)  $s'_t$ :  $L = 21$ FIG. 7: The low-energy spectra for the flux sectors of the diagonal subgroup  $\mathbb{Z}_2^t$ . (a) shows the momentum sector at  $k = \frac{\pi}{2} \pmod{2\pi}$ ; (b) shows the momentum sector at  $k = \frac{3\pi}{2} \pmod{2\pi}$ . Both anyons are the flux anyons for  $\mathbb{Z}_2^t$ .

resentation corresponds to a dyon, which gives rise to the anyon  $f_{zt}$ .

The corresponding spectra for the  $\mathbb{Z}_2^z$  and  $\mathbb{Z}_2^{zt}$  twists are shown in Fig. 6, where the energy levels are exactly twofold degenerate, suggesting the correspond anyons all have quantum dimension  $d = 2$ . Extracting  $s$  using Eq. (22), we find that flux anyons,  $m_z$ ,  $m_{zt}$ , have topological spin  $s = 0$ , while the dyons,  $f_z$ ,  $f_{zt}$ , have topological spin  $s = \frac{1}{2}$ .

Permuting  $x \leftrightarrow y \leftrightarrow z$  gives the remaining four flux anyons  $m_y$ ,  $m_{yt}$ ,  $m_z$ ,  $m_{zt}$ , and four dyons  $f_y$ ,  $f_{yt}$ ,  $f_z$ ,  $f_{zt}$ . The low-energy spectra are identical due to the exact  $S_3$  symmetry of the Hamiltonian (15). The relevant data for the flux and dyons are summarized in Table VI and Table VII.

## 2. Fluxes and dyons for pure translation symmetry twists

Finally, we twist by the translation symmetry. This is done so by computing the low-energy spectrum for odd  $L$  with PBCs (see Fig. 7), which we interpret as the  $\mathbb{Z}_2^t$  flux sector. Again we choose  $L = 1 \pmod{4}$  without loss

Anyon	$s$	$d$	$L \bmod 4$	$R_x$	$R_y$	$R_z$	$e^{ik}$	irrep
$s_t$	$\frac{1}{4}$	2	1 (or 3)	na	na	$\pm i$	$+i$ (or $+i$ )	$\pi(\mathbb{Z}_2^x \times_\omega \mathbb{Z}_2^z)$
$s'_t$	$\frac{3}{4}$	2	1 (or 3)	na	na	$\pm i$	$-i$ (or $+i$ )	$\pi(\mathbb{Z}_2^x \times_\omega \mathbb{Z}_2^z)$

TABLE VIII: Relevant data for flux anyons of  $\mathbb{Z}_2^t$ .

of generality. All energy levels are twofold degenerate (since they all carry half-integer spins).

The  $\mathbb{Z}_2^t$  flux sector can be further divided into two momentum sectors, located at  $k = \frac{\pi}{2}$  and  $\frac{3\pi}{2} \pmod{2\pi}$ . Each sector has twofold degenerate groundstates, that differ in relative momenta from the reference point  $k_{\text{ref}}$ . As a result, the two anyons from the  $\mathbb{Z}_2^t$  flux sector, both with  $d = 2$ , but one with  $s = \frac{1}{4}$ , the other with  $s = \frac{3}{4}$ . We label the one with  $s = \frac{1}{4}$  as  $s_t$  and the one with  $s = \frac{3}{4}$  as  $s'_t$ . This convention is adopted since their topological spin suggests that they correspond to anyons with semionic statistics. The relevant data for the flux anyons are summarized in Table VIII.

This completes our classifications of all sectors from irreducible representations and twists of the symmetry.



Anyon	$\mathbb{1}$	$e_x$	$e_y$	$e_z$	$e_t$	$e_{tx}$	$e_{ty}$	$e_{tz}$	$m_x$	$m_y$	$m_z$	$m_{xt}$	$m_{yt}$	$m_{zt}$	$f_x$	$f_y$	$f_z$	$f_{xt}$	$f_{yt}$	$f_{zt}$	$s_t$	$s'_t$
$s$	0	0	0	0	0	0	0	0	0	0	0	0	0	0	$\frac{1}{2}$	$\frac{1}{2}$	$\frac{1}{2}$	$\frac{1}{2}$	$\frac{1}{2}$	$\frac{1}{2}$	$\frac{1}{4}$	$\frac{3}{4}$
$d$	1	1	1	1	1	1	1	1	2	2	2	2	2	2	2	2	2	2	2	2	2	2

TABLE IX: Anyon data summary.

We have identified all possibly distinct anyon types from the low-energy spectra. The relevant data for anyons and their sectors are shown in Tables V–VIII. For these tables, the column  $e^{ik}$  indicates the momentum sector, instead of the momentum of a specific state. We next assemble this data to pin down the symTO.

### C. Matching with SymTO $\mathcal{D}(D_8)$

We tabulate all 22 low-energy sectors and their corresponding anyon labels in Table IX. To identify the corresponding topological order, we note that any qualifying topological order should have 8 Abelian anyons that correspond to the charges of for  $G_{\text{IR}} = \mathbb{Z}_2^x \times \mathbb{Z}_2^z \times \mathbb{Z}_2^{xzt}$ . Here, it is more convenient to choose the generators of  $G_{\text{IR}}$  to be those of  $\mathbb{Z}_2^x$ ,  $\mathbb{Z}_2^z$ , and  $\mathbb{Z}_2^{xzt}$  subgroups rather than  $\mathbb{Z}_2^x$ ,  $\mathbb{Z}_2^z$ , and  $\mathbb{Z}_2^{xzt}$ , because as we shall see in Sec. V there will be a useful symTO automorphism permuting the corresponding flux anyons  $m_x, m_z, m_{yt}$ . Those 8 Abelian anyons form a symmetric fusion category. We know that the quantum double of  $G_{\text{IR}} = \mathbb{Z}_2^x \times \mathbb{Z}_2^z \times \mathbb{Z}_2^{xzt}$  will have 8 Abelian anyons that form a symmetric fusion category  $\text{Rep}(\mathbb{Z}_2^x \times \mathbb{Z}_2^z \times \mathbb{Z}_2^{xzt})$ . But such a quantum double has 64 anyons instead of the expected 22. The quantum double of  $G_{\text{IR}}$  twisted by a cocycle

$$[\nu] \in H^3(\mathbb{Z}_2^x \times \mathbb{Z}_2^z \times \mathbb{Z}_2^{xzt}, U(1)) \quad (25)$$

also has 8 Abelian anyons that form a symmetric fusion category  $\text{Rep}(\mathbb{Z}_2^x \times \mathbb{Z}_2^z \times \mathbb{Z}_2^{xzt})$ . We thus identify the anyon data above as precisely matching that of the twisted quantum double  $\mathcal{D}^\nu(\mathbb{Z}_2^x \times \mathbb{Z}_2^z \times \mathbb{Z}_2^{xzt})$ , defined by the type-III cocycle, or equivalently, the quantum double of  $D_8$  group (*i.e.* the group of all symmetries of the square), denoted by  $\mathcal{D}(D_8)$ .

Having established that  $G_{\text{IR}} = \mathbb{Z}_2^x \times \mathbb{Z}_2^z \times \mathbb{Z}_2^{xzt}$  is endowed with a type-III anomaly among the three  $\mathbb{Z}_2$  components, we now clarify how this anomaly fixes the emanant symmetry groups and their irreps in the flux sec-

tors. The type-III anomaly in  $G_{\text{IR}}$  implies that whenever a single  $\mathbb{Z}_2$  flux is threaded, the remaining  $\mathbb{Z}_2 \times \mathbb{Z}_2$  subgroup carries a 2D projective representation (rep) within the flux sector. This matches the result from Section III D. We denote such a group by the shorthand

$$\mathbb{Z}_2 \times_\omega \mathbb{Z}_2, \quad (26)$$

for which the representative 2-cocycle is  $\omega$  of the nontrivial second cohomology class  $[\omega] \in H^2(\mathbb{Z}_2 \times \mathbb{Z}_2; \mathbb{R}/\mathbb{Z}) \cong \mathbb{Z}_2$ . The algebra  $\mathbb{Z}_2 \times_\omega \mathbb{Z}_2$  admits exactly one irrep that is compatible with the nontrivial projective phase  $\omega$ , *i.e.*, a 2D projective irrep in which the generators act as Pauli matrices.

This statement can be repackaged equivalently as follows. The cocycle  $\omega$  is trivialized by the minimal central extension

$$1 \rightarrow \mathbb{Z}_2 \rightarrow D_8 \rightarrow \mathbb{Z}_2 \times \mathbb{Z}_2 \rightarrow 1, \quad (27)$$

so that projective irrep of  $\mathbb{Z}_2 \times \mathbb{Z}_2$  is nothing but the unfaithful realization of the 2D irrep for group  $D_8$ . Since  $D_8$  is not represented faithfully, none of its 1D irreps appear. This corresponds to the fact that in the low-energy spectrum, every energy level is at least twofold degenerate. In other words, when a non-trivial  $\mathbb{Z}_2$  flux is inserted, the entire spectrum can be organized into the 2D projective reps of the remaining  $\mathbb{Z}_2 \times \mathbb{Z}_2$  symmetry.

In Tables VI–VIII, we use  $\pi(\mathbb{Z}_2^i \times_\omega \mathbb{Z}_2^j)$  to denote the projective irrep of the remaining  $\mathbb{Z}_2 \times \mathbb{Z}_2$  after the flux of a third  $\mathbb{Z}_2$  is threaded.

## V. SYMTO $\mathcal{D}(D_8)$ AND NEARBY GAPPED PHASES

Having identified the emergent SymTO  $\mathcal{D}(D_8)$  of the gapless spin- $\frac{1}{2}$  Heisenberg chain, we now employ this symTO to constrain the possible neighboring phases. To this end, we first review the properties of the  $D_8$  quantum double.

### A. $D_8$ quantum double $\mathcal{D}(D_8)$

The  $D_8$  quantum double  $\mathcal{D}(D_8)$  has 22 types of anyons, whose quantum dimensions and topological spins are given by Table IX. Its chiral central charge is  $c = 0$  and its total quantum dimension is  $D^2 = \sum_i d_i^2 = 64$ . Every anyon is self-conjugate. The  $S$ -matrix and the fusion rule of  $D_8$  quantum double are given in Appendix A.

The automorphism group of  $D_8$  quantum double from anyon permutation is given by  $S_4$ , which contains the

following 24 permutations of anyon types

$$\begin{aligned}
&(), \\
&(m_y, m_z)(m_{yt}, m_{zt})(f_{yt}, f_{zt})(f_y, f_z)(e_y, e_z)(e_{yt}, e_{zt}), \\
&(m_y, m_{yt})(m_z, m_{zt})(f_{yt}, f_y)(f_{zt}, f_z)(e_t, e_{xt})(e_{yt}, e_{zt}), \\
&(m_y, m_{zt})(m_z, m_{yt})(f_{yt}, f_z)(f_{zt}, f_y)(e_y, e_z)(e_t, e_{xt}), \\
&(m_x, m_y)(m_{xt}, m_{yt})(f_{xt}, f_{yt})(f_x, f_y)(e_x, e_y)(e_{xt}, e_{yt}), \\
&(m_x, m_y, m_z)(m_{xt}, m_{yt}, m_{zt})(f_{xt}, f_{yt}, f_{zt})(f_x, f_y, f_z)(e_x, e_y, e_z)(e_{xt}, e_{yt}, e_{zt}), \\
&(m_x, m_y, m_{xt}, m_{yt})(m_z, m_{zt})(f_{xt}, f_{yt}, f_x, f_y)(f_{zt}, f_z)(e_x, e_y)(e_t, e_{yt}, e_{zt}, e_{xt}), \\
&(m_x, m_y, m_{zt})(m_z, m_{xt}, m_{yt})(f_{xt}, f_{yt}, f_z)(f_{zt}, f_x, f_y)(e_x, e_y, e_z)(e_t, e_{yt}, e_{xt}), \\
&(m_x, m_z, m_y)(m_{xt}, m_{zt}, m_{yt})(f_{xt}, f_{zt}, f_{yt})(f_x, f_z, f_y)(e_x, e_z, e_y)(e_{xt}, e_{zt}, e_{yt}), \\
&(m_x, m_z)(m_{xt}, m_{zt})(f_{xt}, f_{zt})(f_x, f_z)(e_x, e_z)(e_{xt}, e_{zt}), \\
&(m_x, m_z, m_{yt})(m_y, m_{xt}, m_{zt})(f_{xt}, f_{zt}, f_y)(f_{yt}, f_x, f_z)(e_x, e_z, e_y)(e_t, e_{zt}, e_{xt}), \\
&(m_x, m_z, m_{xt}, m_{zt})(m_y, m_{yt})(f_{xt}, f_{zt}, f_x, f_z)(f_{yt}, f_y)(e_x, e_z)(e_t, e_{zt}, e_{yt}, e_{xt}), \\
&(m_x, m_{xt})(m_z, m_{zt})(f_{xt}, f_x)(f_{zt}, f_z)(e_t, e_{yt})(e_{xt}, e_{zt}), \\
&(m_x, m_{xt})(m_y, m_z, m_{yt}, m_{zt})(f_{xt}, f_x)(f_{yt}, f_{zt}, f_y, f_z)(e_y, e_z)(e_t, e_{zt}, e_{xt}, e_{yt}), \\
&(m_x, m_{xt})(m_y, m_{yt})(f_{xt}, f_x)(f_{yt}, f_y)(e_t, e_{zt})(e_{xt}, e_{yt}), \\
&(m_x, m_{xt})(m_y, m_{zt}, m_{yt}, m_z)(f_{xt}, f_x)(f_{yt}, f_z, f_y, f_{zt})(e_y, e_z)(e_t, e_{yt}, e_{xt}, e_{zt}), \\
&(m_x, m_{yt}, m_{xt}, m_y)(m_z, m_{zt})(f_{xt}, f_y, f_x, f_{yt})(f_{zt}, f_z)(e_x, e_y)(e_t, e_{xt}, e_{zt}, e_{yt}), \\
&(m_x, m_{yt}, m_{zt})(m_y, m_z, m_{xt})(f_{xt}, f_y, f_z)(f_{yt}, f_{zt}, f_x)(e_x, e_y, e_z)(e_t, e_{zt}, e_{yt}), \\
&(m_x, m_{yt})(m_y, m_{xt})(f_{xt}, f_y)(f_{yt}, f_x)(e_x, e_y)(e_t, e_{zt}), \\
&(m_x, m_{yt}, m_z)(m_y, m_{zt}, m_{xt})(f_{xt}, f_y, f_{zt})(f_{yt}, f_z, f_x)(e_x, e_y, e_z)(e_t, e_{xt}, e_{zt}), \\
&(m_x, m_{zt}, m_y)(m_z, m_{yt}, m_{xt})(f_{xt}, f_z, f_{yt})(f_{zt}, f_y, f_x)(e_x, e_z, e_y)(e_t, e_{xt}, e_{yt}), \\
&(m_x, m_{zt})(m_z, m_{xt})(f_{xt}, f_z)(f_{zt}, f_x)(e_x, e_z)(e_t, e_{yt}), \\
&(m_x, m_{zt}, m_{yt})(m_y, m_{xt}, m_z)(f_{xt}, f_z, f_y)(f_{yt}, f_x, f_{zt})(e_x, e_z, e_y)(e_t, e_{yt}, e_{zt}), \\
&(m_x, m_{zt}, m_{xt}, m_z)(m_y, m_{yt})(f_{xt}, f_z, f_x, f_{zt})(f_{yt}, f_y)(e_x, e_z)(e_t, e_{xt}, e_{yt}, e_{zt}),
\end{aligned} \tag{28}$$

where each line corresponds to an element of  $S_4$  and each paranthesis corresponds to a cyclic permutation of anyon types inside. The automorphism of the symTO in general does not correspond to a symmetry of the Hamiltonian (15). Thus, in the XYZ limit where various anisotropy terms are nonzero, there is no emergent  $S_4$  symmetry. However, we will later argue that when we restore the full  $SO(3)$  spin rotation symmetry, the  $S_4$  automorphism will become an emergent symmetry. In fact, the emergent symmetry in this case contains  $SO(4)$ , and  $S_4$  as a subgroup of  $SO(4)$ .

The  $D_8$  quantum double has 11 Lagrangian condensable algebras given by the following composite anyons:

$$\begin{aligned}
\mathcal{A}_{1,1} &= 1 \oplus e_x \oplus e_y \oplus e_z \oplus e_t \oplus e_{xt} \oplus e_{yt} \oplus e_{zt} \\
\mathcal{A}_{2,1} &= 1 \oplus m_x \oplus m_y \oplus m_z \oplus e_t \\
\mathcal{A}_{2,2} &= 1 \oplus m_x \oplus m_{yt} \oplus m_{zt} \oplus e_{xt} \\
\mathcal{A}_{2,3} &= 1 \oplus m_y \oplus m_{xt} \oplus m_{zt} \oplus e_{yt} \\
\mathcal{A}_{2,4} &= 1 \oplus m_z \oplus m_{xt} \oplus m_{yt} \oplus e_{zt} \\
\mathcal{A}_{3,1} &= 1 \oplus 2m_x \oplus e_x \oplus e_t \oplus e_{xt} \\
\mathcal{A}_{3,2} &= 1 \oplus 2m_y \oplus e_y \oplus e_t \oplus e_{yt} \\
\mathcal{A}_{3,3} &= 1 \oplus 2m_z \oplus e_z \oplus e_t \oplus e_{zt}
\end{aligned}$$

$$\begin{aligned}
\mathcal{A}_{3,4} &= 1 \oplus 2m_{xt} \oplus e_x \oplus e_{yt} \oplus e_{zt} \\
\mathcal{A}_{3,5} &= 1 \oplus 2m_{yt} \oplus e_y \oplus e_{xt} \oplus e_{zt} \\
\mathcal{A}_{3,6} &= 1 \oplus 2m_{zt} \oplus e_z \oplus e_{xt} \oplus e_{yt}
\end{aligned} \tag{29}$$

The Lagrangian condensable algebras are divided into three classes. The condensable algebras in the same class are connected by the  $S_4$  automorphisms.

The Heisenberg chain has a  $SO(3)$  spin rotation plus a lattice translation symmetry, with each lattice site carrying a spinor representation of  $SO(3)$ . If we restrict ourselves to the  $\mathbb{Z}_2^x \times \mathbb{Z}_2^z$  subgroup of the full  $SO(3)$  and the lattice translation symmetry, the symTO of the Heisenberg chain is found to be the quantum double of  $D_8$ , with the topological symmetry boundary induced by the condensation of the following Lagrangian condensable algebra:

$$\mathcal{A}_{1,1} = 1 \oplus e_x \oplus e_y \oplus e_z \oplus e_t \oplus e_{xt} \oplus e_{yt} \oplus e_{zt}. \tag{30}$$

The 22 anyons in the  $D_8$  quantum double correspond to 22 low energy sectors of the Heisenberg chain, which are obtained via the irreps of emanant symmetry groups for various symmetry twists of spin rotations and translation (see Section IV).

From Section IV, taking into account anyon quantum dimensions, their self/mutual statistics, fusion rules, and the action of the automorphisms, we can identify anyons in  $\mathcal{D}_8$  with the symmetry charges and defects of the spin rotation and translation:

1.  $e_x, e_y, e_z$  anyons carry the  $\mathbb{Z}_2$  charges of  $S_x$   $\pi$ -rotation  $R_x$ ,  $S_y$   $\pi$ -rotation  $R_y$ , and  $S_z$   $\pi$ -rotation  $R_z$ . The three transformations are not independent:  $R_x R_y = (-1)^L R_z$  and  $R_x R_z = (-1)^L R_y$ . In fact,  $e_x, e_y, e_z$  anyons are created by the spin operators  $\sigma_j^x, \sigma_j^y, \sigma_j^z$ , respectively. Thus  $e_x$  anyon carry non-trivial  $\mathbb{Z}_2$  charges of  $R_y$  and  $R_z$ . As a result, if  $e_x$  anyon condenses, it will create a ferromagnetic phase with order parameter  $\langle \sigma_j^x \rangle = s \neq 0$ .

$e_x, e_y, e_z$  anyons correspond to  $R_x, R_y, R_z = \pm 1$  and momentum-0 sectors on a ring of size 0 mod 4 (see Fig. 5(b,c,d)).

2.  $e_t$  anyon carries  $\pi$  crystal momentum (*i.e.* the  $\mathbb{Z}_2$  charge from translation). It is created by spin-singlet operator  $(-1)^j$  (where  $j$  labels lattice sites). Thus if  $e_t$  anyon condenses, it will break the  $j \rightarrow j+1$  translation symmetry, but preserve the  $j \rightarrow j+2$  translation symmetry.

$e_t$  anyon corresponds to  $R_x, R_y, R_z = 1$  and momentum- $\pi$  sector on a ring of size 0 mod 4 (see Fig. 5(e)).

3. Trivial  $\mathbb{1}$  anyon corresponds to  $R_x, R_y, R_z = 1$  and momentum-0 sector on a ring of size 0 mod 4 (see Fig. 5(a)).

4.  $e_{xt}, e_{yt}, e_{zt}$  anyons are created by staggered spin operators  $(-1)^j \sigma_j^x, (-1)^j \sigma_j^y, (-1)^j \sigma_j^z$ , respectively. If  $e_{xt}$  anyon condenses, it will create an anti-ferromagnetic phase with  $\langle \sigma_j^x \rangle = \pm (-1)^j s_x \neq 0$ .

$e_{xt}, e_{yt}, e_{zt}$  anyons correspond to  $R_x, R_y, R_z = \pm 1$  and momentum- $\pi$  sectors on a ring of size 0 mod 4 (see Fig. 5(f,g,h)).

5.  $m_x, m_y, m_z$  anyons correspond to the symmetry twists of  $S_x$   $\pi$ -rotation,  $S_y$   $\pi$ -rotation, and  $S_z$   $\pi$ -rotation, respectively. Due to the type-III mixed anomaly between the spin  $\pi$ -rotations and translation, those symmetry twists carry spin and translation quantum numbers. From the fusion  $m_x \otimes m_x = \mathbb{1} \oplus e_z \oplus e_t \oplus e_{zt}$ , we see that the bound state of two  $S_x$   $\pi$ -rotation symmetry twists carries  $S_y$  and  $S_z$  quantum numbers, as well as  $\pi$  crystal momentum.

$m_x, m_y, m_z$  anyons correspond to momentum-0 sectors on a ring of size 0 mod 4 with twisted boundary condition generated by  $S_x$   $\pi$ -rotation,  $S_y$   $\pi$ -rotation, and  $S_z$   $\pi$ -rotation, respectively (see Fig. 6(a)).

6. We note the  $e_t$  anyon has trivial mutual statistics with anyons  $e_x, e_y, e_z, e_t, e_{xt}, e_{yt}, e_{zt}, m_x, m_y, m_z, f_x, f_y, f_z$ , according to the  $S$ -matrix. Thus those

anyons do not contain symmetry twist of translation. On the other hand, the  $e_t$  anyon has  $\pi$  mutual statistics with anyons  $s_t, s'_t, m_{xt}, m_{yt}, m_{zt}, f_{xt}, f_{yt}, f_{zt}$ . Thus those anyons contain symmetry twist of translation. Also, anyons  $m_{xt}, m_{yt}, m_{zt}, f_{xt}, f_{yt}, f_{zt}$  has non-trivial mutual statistics with anyons  $e_x, e_y, e_z$ , indicating that anyons  $m_{xt}, m_{yt}, m_{zt}, f_{xt}, f_{yt}, f_{zt}$  also contain symmetry twist of spin rotation. On the other hand, anyons  $s_t, s'_t$  has trivial mutual statistics with anyons  $e_x, e_y, e_z$ . Thus anyons  $s_t, s'_t$  are pure symmetry twist of translation.  $s_t$  and  $s'_t$  differ by a crystal momentum  $\pi$  (*i.e.* differ by a  $e_t$ -anyon).

Since  $s_t$  is the translation-symmetry twist, any translation symmetric gapped states must have  $s_t$  condensation. Since  $s_t$  is a semion, which cannot condense, thus any gapped states must break translation symmetry. The fractional statistics of  $s_t$  anyon also indicates a self anomaly of the  $j \rightarrow j+1$  translation symmetry.

$s_t, s'_t$  anyons correspond to momentum- $\pm\pi/2$  sectors on a ring of size  $\pm 1$  mod 4 (see Fig. 7(c)).

7. From  $s_t \otimes m_x = m_{xt} \oplus f_{xt}$ , we see that anyons  $m_{xt}, f_{xt}$  are symmetry twist of  $S_x$ -rotation and translation.  $m_{xt}$  and  $f_{xt}$  differ by  $\pi$  crystal momentum (*i.e.* by a  $e_t$ -anyon). Similarly, anyons  $m_{yt}, f_{yt}$  ( $m_{zt}, f_{zt}$ ) are symmetry twist of  $S_y$ -rotation ( $S_z$ -rotation) and translation.

$m_{xt}, m_{yt}, m_{zt}, (f_{xt}, f_{yt}, f_{zt})$  anyons correspond to momentum-0 (momentum- $\pi$ ) sectors on a ring of size  $\pm 1$  mod 4 with twisted boundary condition generated by  $S_x$   $\pi$ -rotation,  $S_y$   $\pi$ -rotation, and  $S_z$   $\pi$ -rotation, respectively (see Fig. 6(c)).

8. From the fusion, we see that anyons  $f_x, f_y, f_z$  are symmetry twists of  $S_x$   $\pi$ -rotation,  $S_y$   $\pi$ -rotation, and  $S_z$   $\pi$ -rotation, plus additional spin quantum numbers.

$f_x, f_y, f_z$  anyons correspond states on a ring of size 0 mod 4 with twisted boundary condition generated by  $S_x$   $\pi$ -rotation,  $S_y$   $\pi$ -rotation, and  $S_z$   $\pi$ -rotation, respectively (see Fig. 6(b)).

We see that the topological symmetry boundary is obtained by condensing all the symmetry charges of spin rotations and translation, as expected.

The gapped phases of Heiberg chain with reduced symmetry of  $S_x, S_y, S_z$   $\pi$ -rotations and translation are classified by the 11 Lagrangian condensable algebra  $\mathcal{A}$  of the symTO  $\mathcal{D}(D_8)$ . Those 11 gapped phases are obtained by condensing anyons in the corresponding condensable algebra  $\mathcal{A}$ , which can be grouped into three classes by automorphisms of the symTO:

$$\left\{ (\mathcal{A}_{2,1}, \mathcal{A}_{2,2}, \mathcal{A}_{2,3}, \mathcal{A}_{2,4})_2^{\text{SSB}} \right\},$$

$$\left\{ (\mathcal{A}_{3,1}, \mathcal{A}_{3,2}, \mathcal{A}_{3,3}, \mathcal{A}_{3,4}, \mathcal{A}_{3,5}, \mathcal{A}_{3,6})_4^{\text{SSB}} \right\},$$

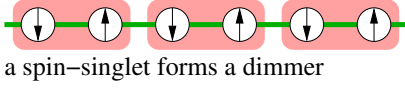


FIG. 8: The dimmer phase of a spin chain (from condensable algebra  $\mathcal{A}_{2,1}$ ).



FIG. 9: The anti-ferromagnetic phase of a spin chain (from condensable algebra  $\mathcal{A}_{2,2}, \mathcal{A}_{2,3}, \mathcal{A}_{2,4}$ ).

$$\left\{ (\mathcal{A}_{1,1})_8^{\text{SSB}} \right\}, \quad (31)$$

All those phases have spontaneous symmetry breaking (SBB), and the subscript correspond to the ground state degeneracy of the gapped phases.

The phase- $\mathcal{A}_{2,1}$  is induced by the condensation of  $\mathcal{A}_{2,1} = 1 \oplus m_x \oplus m_y \oplus m_z \oplus e_t$ . The condensations of the symmetry twists  $m_x, m_y, m_z$  of  $S_x, S_y, S_z$   $\pi$ -rotations indicate that the phase- $\mathcal{A}_{2,1}$  is symmetric under the  $S_x, S_y, S_z$   $\pi$ -rotations. The condensation of  $e_t$  anyon indicate that the phase- $\mathcal{A}_{2,1}$  breaks the translation symmetry spontaneously. Thus, the phase- $\mathcal{A}_{2,1}$  is the spin-singlet dimer phase (see Fig. 8).

The phase- $\mathcal{A}_{2,2}$  is induced by the condensation of  $\mathcal{A}_{2,2} = 1 \oplus m_x \oplus m_{yt} \oplus m_{zt} \oplus e_{xt}$ . The condensations of the symmetry twists  $m_x$ , indicate that the phase- $\mathcal{A}_{2,2}$  is symmetric under the  $S_x$   $\pi$ -rotations. The condensations of the symmetry twists  $V, W$ , indicate that the phase- $\mathcal{A}_{2,2}$  is symmetric under the  $S_y, S_z$   $\pi$ -rotations followed by a translation. The condensation of  $e_{xt}$  anyon indicate that the phase- $\mathcal{A}_{2,2}$  has the following order parameter  $\langle \sigma_j^x \rangle = (-1)^j s$ ,  $\langle \sigma_j^y \rangle = 0$ ,  $\langle \sigma_j^z \rangle = 0$ . Thus, the phase- $\mathcal{A}_{2,2}$  is the anti-ferromagnetic phase with spins in  $x$ -direction. Similarly, the phase- $\mathcal{A}_{2,3}$  (phase- $\mathcal{A}_{2,4}$ ) is the anti-ferromagnetic phase with spins in  $y$ -direction ( $z$ -direction, see Fig. 9).

The phase- $\mathcal{A}_{3,1}$  is induced by the condensation of  $\mathcal{A}_{3,1} = 1 \oplus 2m_x \oplus e_x \oplus e_t \oplus e_{xt}$ . Compare to the phase- $\mathcal{A}_{2,2}$  where  $e_{xt}$  condenses leading to  $\langle \sigma_j^x \rangle = (-1)^j s$ , there is an additional condensation of  $e_x$ . The condensation of  $x, u$  lead to  $\langle \sigma_j^x \rangle = s' + (-1)^j s$ . We also have  $\langle \sigma_j^y \rangle = 0$ ,  $\langle \sigma_j^z \rangle = 0$  since  $m_x$  condenses indicating  $S_x$   $\pi$ -rotation symmetry. Thus, the phase- $\mathcal{A}_{3,1}$  is a ferromagnetic phase with spins in  $x$ -direction which also breaks the translation symmetry (see Fig. 10).

The phase- $\mathcal{A}_{3,4}$  is induced by the condensation of  $\mathcal{A}_{3,4} = 1 \oplus 2m_{xt} \oplus e_x \oplus e_{yt} \oplus e_{zt}$ . The condensation of  $x, v, w$  lead to  $\langle \sigma_j^x \rangle = s_x$ ,  $\langle \sigma_j^y \rangle = (-1)^j s_y$ ,  $\langle \sigma_j^z \rangle = (-1)^j s_z$ .  $m_{xt}$  condensation implies a symmetry of  $S_x$   $\pi$ -rotation followed by a  $j \rightarrow j+1$  translation. Thus, the phase- $\mathcal{A}_{3,4}$  is a phase with ferromagnetic order for spins in  $x$ -direction and anti-ferromagnetic order for spins in  $y, z$ -direction (see Fig. 11).

The phase- $\mathcal{A}_{1,1}$  is induced by the condensation of  $\mathcal{A}_{1,1} = 1 \oplus e_x \oplus e_y \oplus e_z \oplus e_t \oplus e_{xt} \oplus e_{yt} \oplus e_{zt}$ . The con-



FIG. 10: A collinear ferromagnetic phase of a spin chain, that also breaks translation symmetry (from condensable algebra  $\mathcal{A}_{3,1}, \mathcal{A}_{3,2}, \mathcal{A}_{3,3}$ ).



FIG. 11: A phase of a spin chain, with ferromagnetic order for spins in  $x$ -direction and anti-ferromagnetic order for spins in  $y$ -direction (from condensable algebra  $\mathcal{A}_{3,4}, \mathcal{A}_{3,5}, \mathcal{A}_{3,6}$ ).

densation of all the charges leads to  $\langle \sigma_j^x \rangle = s'_x + (-1)^j s_x$ ,  $\langle \sigma_j^y \rangle = s'_y + (-1)^j s_y$ ,  $\langle \sigma_j^z \rangle = s'_z + (-1)^j s_z$ . Thus, the phase- $\mathcal{A}_{1,1}$  is a ferromagnetic phase with non-collinear spins which also breaks the translation symmetry (see Fig. 12).

## VI. $SO(4)$ REPRESENTATION OF 2d SPT AND ITS CONNECTION TO 1d SPIN CHAIN

Our numerical calculation for spin- $\frac{1}{2}$  Heisenberg chain reveals an emergent  $S_4$  symmetry, in addition to the  $SO(3)$  spin rotation and translation symmetry. This emergent  $S_4$  symmetry suggests an emergent  $SO(4)$  symmetry of the spin- $\frac{1}{2}$  Heisenberg chain.

To see the emergent  $SO(4)$  symmetry, here we mostly follow the nonlinear  $\sigma$ -model (NL $\sigma$ M) description of a class of SPT states in Ref. [101–103]. For those 2d SPT states, this description has a manifest maximal “parent”  $SO(4)$  symmetry. Many SPT states can be viewed as descendants of this description. We will draw connection of the 1d boundary of the SPT state to spin-1/2 chain.

The bulk description of the  $SO(4)$  SPT state is

$$\mathcal{S}_{2d} = \int d\tau d^2x \frac{(\partial \vec{\phi})^2}{g^2} + \frac{i2\pi}{\Omega_3} \epsilon_{abcd} \phi_a \partial_\tau \phi_b \partial_x \phi_c \partial_y \phi_d. \quad (32)$$

Here  $\vec{\phi} = (\phi_1, \phi_2, \phi_3, \phi_4)$  is a unit  $SO(4)$  vector. The 1d boundary of this state is (see also [104])

$$\mathcal{S}_{1d} = \int d\tau dx \frac{1}{g} (\partial \vec{\phi})^2 + \int_{u=0}^1 du \frac{i2\pi}{\Omega_3} \epsilon_{abcd} \phi_a \partial_\tau \phi_b \partial_x \phi_c \partial_u \phi_d. \quad (33)$$

The boundary theory has an  $SO(4)$  anomaly  $(k_R, k_L) = (1, -1)$  mentioned in the introduction.

It is known that the  $(1+1)d$  NL $\sigma$ M with a WZW term flows to a CFT fixed point  $g = g^*$ . At this fixed point, the  $SO(4)$  symmetry factorizes into  $SU(2)_L$  and  $SU(2)_R$  symmetries [104]. To see the  $SU(2)_L \times SU(2)_R$  symmetry, we can define a matrix field  $\Phi$  as

$$\Phi = \phi_4 \sigma^0 + i\phi_1 \sigma^1 + i\phi_2 \sigma^2 + i\phi_3 \sigma^3, \quad (34)$$

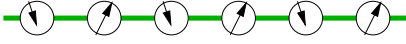


FIG. 12: A ferromagnetic phase of a spin chain, with non-collinear spins which also breaks the translation symmetry (from condensable algebra  $\mathcal{A}_{1,1}$ ).

$$SU(2)_L \times SU(2)_R : \Phi \rightarrow U_L \Phi U_R^\dagger. \quad (35)$$

Both  $U_L$  and  $U_R$  are both  $SU(2)$  matrices.

We can use the SPT order realized by the CZX model [105] as an example. This state correspond to the  $NL\sigma M$  models above, with the following  $\mathbb{Z}_2$  symmetry:

$$\mathbb{Z}_2 : \vec{\phi} \rightarrow -\vec{\phi}. \quad (36)$$

Hence although the 1d boundary is nonchiral, only the right-moving modes carry the  $\mathbb{Z}_2$  charge. This CZX  $\mathbb{Z}_2$  is the center of  $SU(2)_R$ , and it plays the same role as the translation of the spin-1/2 chain.

The field theory Eq. (33) also describes the 1d spin-1/2 chain, with the following identification between the order parameter and the fields:

$$\vec{\phi} \sim (n_x, n_y, n_z, V), \quad (37)$$

where  $\vec{n} = (n_x, n_y, n_z)$  is the Neel order vector, and  $V$  is the VBS order parameter. Under translation by one lattice constant, both Neel and VBS order parameter change sign, hence  $T : \vec{\phi} \rightarrow -\vec{\phi}$ .

We can discuss multiple  $\mathbb{Z}_2$  subgroups of  $SO(4)$  in Eq. (32) and Eq. (33):

$$\begin{aligned} \mathbb{Z}_2^z : n_x \rightarrow -n_x, n_y \rightarrow -n_y, n_z \rightarrow n_z, V \rightarrow V; \\ \mathbb{Z}_2^x : n_x \rightarrow n_x, n_y \rightarrow -n_y, n_z \rightarrow -n_z, V \rightarrow V; \\ \mathbb{Z}_2^{yt} : n_x \rightarrow n_x, n_y \rightarrow -n_y, n_z \rightarrow n_z, V \rightarrow -V. \end{aligned} \quad (38)$$

$\mathbb{Z}_2^z$  and  $\mathbb{Z}_2^x$  are subgroup of spin- $SO(3)$ , in particular they are the  $\pi$ -rotation about the  $z$  and  $x$  axis.  $\mathbb{Z}_2^{yt}$  is the combination of translation  $T$  and  $\mathbb{Z}_2^y$ . The advantage of grouping symmetries this way is that, the three  $\mathbb{Z}_2$ s are related by the  $SO(4)$  symmetry, as well as an automorphism of  $\mathcal{D}(D_8)$ :

$$\begin{aligned} (m_x, m_z, m_{yt})(m_y, m_{xt}, m_{zt})(f_{xt}, f_{zt}, f_y)(f_{yt}, f_x, f_z) \\ (e_x, e_z, e_y)(e_t, e_{zt}, e_{xt}). \end{aligned} \quad (39)$$

In other words, the  $\mathbb{Z}_2^z$ ,  $\mathbb{Z}_2^x$ , and  $\mathbb{Z}_2^{yt}$  symmetry transformation correspond to the symmetry-defects  $m_x, m_z, m_{yt}$ . We remark that there is no “self-anomaly” of these  $\mathbb{Z}_2$ s, but there is type III mixed anomaly between them. If we view translation  $T$  as a  $\mathbb{Z}_2$  symmetry, it will have self-anomaly, as it plays the same role as the  $\mathbb{Z}_2$  in CZX model.

Also the four transformations related by the  $SO(4)$  symmetry

$$\mathbb{Z}_2^z : n_x \rightarrow -n_x, n_y \rightarrow -n_y, n_z \rightarrow n_z, V \rightarrow V;$$

$$\begin{aligned} \mathbb{Z}_2^x : n_x \rightarrow n_x, n_y \rightarrow -n_y, n_z \rightarrow -n_z, V \rightarrow V; \\ \mathbb{Z}_2^{zt} : n_x \rightarrow n_x, n_y \rightarrow n_y, n_z \rightarrow -n_z, V \rightarrow -V. \\ \mathbb{Z}_2^{xt} : n_x \rightarrow -n_x, n_y \rightarrow n_y, n_z \rightarrow n_z, V \rightarrow -V. \end{aligned} \quad (40)$$

are also related by another automorphism of  $\mathcal{D}(D_8)$ :

$$\begin{aligned} (m_x, m_{zt}, m_{xt}, m_z)(m_y, m_{yt})(f_{xt}, f_z, f_x, f_{zt}) \\ (f_{yt}, f_y)(e_x, e_z)(e_t, e_{xt}, e_{yt}, e_{zt}) \end{aligned} \quad (41)$$

So the transformations  $\mathbb{Z}_2^z$ ,  $\mathbb{Z}_2^x$ ,  $\mathbb{Z}_2^{zt}$ , and  $\mathbb{Z}_2^{xt}$  correspond to the symmetry defects  $m_x, m_{zt}, m_{xt}, m_z$ . We see that the  $S_4$  automorphism of  $\mathcal{D}(D_8)$  is part of  $SO(4)$  symmetry.

We can create a defect of translation  $T$ . This defect will carry a spin-1/2 excitation (compatible with the numerical result of the difference between odd and even lengths), which is precisely the  $CP^1$  field  $z_\alpha$ :

$$\vec{n} = z^\dagger \vec{\sigma} z. \quad (42)$$

Under translation  $T$  and  $\mathbb{Z}_2^{yt}$ ,  $z$  transforms as

$$T : z \rightarrow i\sigma^y z^*, \quad \mathbb{Z}_2^{yt} : z \rightarrow z^*. \quad (43)$$

One can see that when acting on the spinon  $z_\alpha$ ,  $T^2 = -1$ , which is compatible with the numerical result that the spin-1/2 excitation is at momentum  $\pi/2$ .

The  $\mathbb{Z}_2$ s in Eq. (38) do not permute each other. One can also consider other symmetries that do permute them, for example this  $\mathbb{Z}_4$  symmetry:

$$\mathbb{Z}_4 : \phi_1 \rightarrow \phi_4, \phi_2 \rightarrow \phi_3, \phi_3 \rightarrow -\phi_2, \phi_4 \rightarrow -\phi_1. \quad (44)$$

This  $\mathbb{Z}_4$  swaps  $\mathbb{Z}_2^z$  and  $\mathbb{Z}_2^{yt}$  above. Interestingly,  $(\mathbb{Z}_4)^2$  is the same as translation  $T$ .

## VII. GAPLESS CFT BOUNDARY OF SYMTO $\mathcal{D}(D_8)$

The gapless boundary of symTO  $\mathcal{D}(D_8)$  that has no condensation is described by multi component partition function  $\chi_a^{\mathcal{D}(D_8)}(\tau, \bar{\tau})$ , where  $a$  label the 22 types of anyons of  $D_8$  quantum double  $\mathcal{D}(D_8)$ .  $\chi_a^{\mathcal{D}(D_8)}(\tau, \bar{\tau})$  transforms according to the  $S, T$  matrix of  $\mathcal{D}(D_8)$

$$\begin{aligned} \chi_a^{\mathcal{D}(D_8)}(-1/\tau, -1/\bar{\tau}) &= D^{-1} S_{ab}^{\mathcal{D}(D_8)} \chi_b^{\mathcal{D}(D_8)}(\tau, \bar{\tau}) \\ \chi_a^{\mathcal{D}(D_8)}(\tau + 1, \bar{\tau} + 1) &= T_{ab}^{\mathcal{D}(D_8)} \chi_b^{\mathcal{D}(D_8)}(\tau, \bar{\tau}) \end{aligned} \quad (45)$$

However, we do not know which conformal field theory (CFT) gives rise to the partition function  $\chi_a^{\mathcal{D}(D_8)}(\tau, \bar{\tau})$  where all components are non-zero.

On the other hand, the gapless phase of Heisenberg chain is described by  $SU(2)$  level-1 Kac-Moody algebra  $su_{21} \times su_{21}$ . The  $su_{21} \times su_{21}$  CFT is described by a 4-component partition function  $\chi_\alpha^{su_{21} \times su_{21}}(\tau, \bar{\tau})$ ,



which transforms according to the  $S, T$  matrices of double-semion topological order. where  $\alpha \in \{(1, 1), (1, \bar{s}), (s, 1), (s, \bar{s})\}$  labels the anyons in the double-semion topological order. We find that the two partition functions must have the following relation

$$\begin{aligned}\chi_{1,0;\bar{1},0}^{su2_1 \times \overline{su2_1}} &= \chi_{1,0}^{\mathcal{D}(D_8)} + \chi_{e_x,0}^{\mathcal{D}(D_8)} + \chi_{e_y,0}^{\mathcal{D}(D_8)} + \chi_{e_z,0}^{\mathcal{D}(D_8)} \\ \chi_{1,0;\bar{s},-\frac{1}{4}}^{su2_1 \times \overline{su2_1}} &= 2\chi_{s',\frac{3}{4}}^{\mathcal{D}(D_8)} \\ \chi_{s,\frac{1}{4};\bar{1},0}^{su2_1 \times \overline{su2_1}} &= 2\chi_{s,\frac{1}{4}}^{\mathcal{D}(D_8)} \\ \chi_{s,\frac{1}{4};\bar{s},-\frac{1}{4}}^{su2_1 \times \overline{su2_1}} &= \chi_{e_t,0}^{\mathcal{D}(D_8)} + \chi_{e_{xt},0}^{\mathcal{D}(D_8)} + \chi_{e_{yt},0}^{\mathcal{D}(D_8)} + \chi_{e_{zt},0}^{\mathcal{D}(D_8)}\end{aligned}\quad (46)$$

In other words, the modular covariance of  $\chi_a^{\mathcal{D}(D_8)}(\tau, \bar{\tau})$  ensure the modular covariance of  $\chi_a^{su2_1 \times \overline{su2_1}}(\tau, \bar{\tau})$ , and the above is the only solution where all components of  $\chi_a^{su2_1 \times \overline{su2_1}}(\tau, \bar{\tau})$  are non-zero. The existence of the solution (46) indicates that the  $\mathcal{D}(D_8)$  symTO is consistent with the known result that the gapless Heisenberg chain is described by  $su2_1 \times \overline{su2_1}$  CFT.

### VIII. NEIGHBORING STATES OF SPIN- $\frac{1}{2}$ HEISENBERG CHAIN

In this section, we explore the neighboring states of the gapless phase of  $SO(3)$  symmetric Heisenberg chain described by  $su2_1 \times \overline{su2_1}$  CFT. By neighboring states, we mean to consider only states induced by interactions of low-energy excitations. We assume the high energy excitations at energy scale of spin coupling remain unchanged as we change the interactions between low-energy excitations. What kinds of states that can be induced by changing the interactions between low-energy excitations in spin- $\frac{1}{2}$  Heisenberg chain?

If we lower the  $SO(3)$  spin-rotation symmetry to  $S_x, S_y, S_z$   $\pi$ -rotation symmetry, the emanant symmetry of the modified spin- $\frac{1}{2}$  Heisenberg chain is described by symTO  $\mathcal{D}(D_8)$ . If the high energy excitations are not affected, we still have the same symTO  $\mathcal{D}(D_8)$  even if we change the interactions between low-energy excitations. Thus the possible neighboring states of the modified Heisenberg chain are controlled by the emanant symTO  $\mathcal{D}(D_8)$ . In particular, the gaped phases are classified by the Lagrangian condensable algebra of the symTO. We find that there are 11 gapped neighboring phases if we reduce  $SO(3)$  to  $\mathbb{Z}_2^x \times \mathbb{Z}_2^z$ , as discussed before.

From these 11 gapped neighboring phases with reduced symmetry, we can infer the neighboring states for the Heisenberg model with the full  $SO(3)$  spin-rotation symmetry. In this case, there is an emergent  $SO(4)$  symmetry, which contains the exact emanant symTO  $\mathcal{D}(D_8)$  and  $SO(3)$  spin-rotation symmetry. The  $S_4$  automorphism of the symTO  $\mathcal{D}(D_8)$  becomes part of the emergent  $SO(4)$  symmetry.

Before our discussion of neighboring phases, we first review the notions commensurate phase and incommensurate phase for *translation symmetric phases* [106–108].

Naively, if the gapless modes in a phase carry a crystal momentum which is a rational fraction of Brillouin zone size, then the phase is commensurate. Otherwise, the phase is incommensurate. More precisely, we consider the crystal momenta of low-energy many-body excitations created by local operators. If the crystal momenta are commensurate with the Brillouin zone size, then the state is commensurate. Otherwise, the state is incommensurate. An example of incommensurate state is a lattice gas of conserved bosons with incommensurate density. An 1+1D Fermi liquid is incommensurate if  $k_F a / 2\pi$  is irrational, where  $a$  is the unit cell size. A gapped translation symmetric phases are always commensurate.

The three anti-ferromagnetic phases  $\mathcal{A}_{2,2}, \mathcal{A}_{2,3}, \mathcal{A}_{2,4}$  are connected by the restored  $SO(3)$  spin-rotation symmetry. With the full  $SO(3)$  symmetry, those phases spontaneously break a continuous  $SO(3)$  symmetry (without ferromagnetic order), as well as the emergent  $SO(4)$  symmetry. In 1+1D, the quantum fluctuations always restore the symmetry and can give rise to a gapless phase described by the  $su2_1 \times \overline{su2_1}$  CFT. In other words, the three gapped phases  $\mathcal{A}_{2,2}, \mathcal{A}_{2,3}, \mathcal{A}_{2,4}$  for reduced symmetry become a single gapless phase for the restored  $SO(3)$  symmetry. Such a gapless phase has the exact emergent  $SO(4)$  symmetry in zero energy limit.

The gapped dimer phase- $\mathcal{A}_{2,1}$  remains to be a gapped phase after we restore the  $SO(3)$  spin-rotation symmetry (see Fig. 8). However, we note that the dimer phase- $\mathcal{A}_{2,1}$  and the three anti-ferromagnetic phases  $\mathcal{A}_{2,2}, \mathcal{A}_{2,3}, \mathcal{A}_{2,4}$  are connected the  $S_4$  automorphism of the symTO  $\mathcal{D}(D_8)$ . Thus, they are connected by the emergent  $SO(4)$  symmetry. Therefore, the  $\mathcal{A}_{2,1}, \mathcal{A}_{2,2}, \mathcal{A}_{2,3}, \mathcal{A}_{2,4}$  phases spontaneously break the emergent  $SO(4)$  symmetry. The dimer phase would have a linear gapless mode from the spontaneous  $SO(4)$  symmetry breaking if the symmetry was exact. However, the gapless mode can consistently acquire a gap since at the gap scale, the  $SO(4)$  symmetry becomes approximate.

If the quantum fluctuations in the above discussion are very strong, can we get a gapped symmetric state, with the full  $SO(3)$  and translation symmetry? The answer is no. Since the  $SO(3)$  symmetric model has at least the reduced spin rotation symmetry and translation symmetry, we have showed that the gapped symmetric state with the translation symmetry is impossible. However, if the gapped state has only spin rotation symmetry but breaks the translation symmetry, then such a gapped dimer state is possible.

The three co-linear ferromagnetic phases  $\mathcal{A}_{3,1}, \mathcal{A}_{3,2}, \mathcal{A}_{3,3}$  that break the translation symmetry (see Fig. 10) are connected by the restored  $SO(3)$  spin-rotation symmetry. With the full  $SO(3)$  symmetry, those phases spontaneously break a continuous  $SO(3)$  symmetry with a ferromagnetic order. In this case, the quantum fluctuations do not restore the  $SO(3)$  symmetry. Thus we get a  $SO(3)$  SSB phase with quadratic dispersing spin wave  $\omega \sim k^2$ , due to the ferromagnetic order. In other words, the three gapped phases  $\mathcal{A}_{3,1}, \mathcal{A}_{3,2}, \mathcal{A}_{3,3}$  for reduced sym-

metry become a single gapless ferromagnetic phase that breaks the translation symmetry for the restored  $SO(3)$  symmetry.

The three canted anti-ferromagnetic phases  $\mathcal{A}_{3,4}$ ,  $\mathcal{A}_{3,5}$ ,  $\mathcal{A}_{3,6}$  (where the canting induce a ferromagnetic order, see Fig. 11) again are connected by the restored  $SO(3)$  spin-rotation symmetry. To understand the dynamics of such a phase in the presence of the  $SO(3)$  symmetry, we apply a magnetic field to pin the ferromagnetic spin direction. In this case, we still have an anti-ferromagnetic order for spin in the transverse direction and the  $SO(3)$  symmetry is reduced to  $U(1)$  symmetry. The anti-ferromagnetic order for the transverse spin breaks the  $U(1)$  symmetry. But the quantum fluctuations restore the  $U(1)$  symmetry and leads to a gapless translation symmetric phase described by  $u1 \times \bar{u}1$  CFT with linear dispersion  $\omega \sim |k|$ . We stress that such a gapless phase is a commensurate phase due to the anti-ferromagnetic order for the transverse spin.

Now, we remove the pinning magnetic field. The ferromagnetic spin order spontaneously breaks the  $SO(3)$  symmetry down to a  $U(1)$  symmetry. In this case, we expect to have two gapless modes: an anti-ferromagnetic transverse spin mode with linear dispersion  $\omega \sim |k|$ , and a ferromagnetic spin mode with quadratic dispersion  $\omega \sim k^2$ .

The non-co-linear ferromagnetic phase  $\mathcal{A}_{1,1}$  with translation symmetry breaking (see Fig. 12), spontaneously break the  $SO(3)$  symmetry after restoring the symmetry. In the presence of the  $SO(3)$  symmetry, such a phase must be gapless. To understand such a phase, we again apply a magnetic field to pin the ferromagnetic spin direction. In this case, we may have an ferromagnetic order for spin in the transverse direction and the  $SO(3)$  symmetry is reduced to  $U(1)$  symmetry. The ferromagnetic order for the transverse spin breaks the  $U(1)$  symmetry. But the quantum fluctuation restore the  $U(1)$  symmetry and leads to a gapless translation symmetric phase described by  $u1 \times \bar{u}1$  CFT with linear dispersion  $\omega \sim |k|$ . We stress that such a gapless phase is an incommensurate phase due to the ferromagnetic order for the transverse spin. We note that fluctuations of ferromagnetic order for the transverse spin are described by ferromagnetic XY model with a non-zero average  $S_z$ . A ferromagnetic XY model is equivalent to a gas of conserved bosons, where the boson density corresponds to average  $S_z$ . Such a ferromagnetic XY model gives rise to an incommensurate phase.

Now, we remove the pinning magnetic field. The ferromagnetic spin order spontaneously break the  $SO(3)$  symmetry down to a  $U(1)$  symmetry. In this case, we expect to have two gapless modes: an ferromagnetic transverse spin mode with linear dispersion  $\omega \sim |k|$ , and a ferromagnetic spin mode with quadratic dispersion  $\omega \sim k^2$ . Such a gapless phase is an incommensurate phase, due to the ferromagnetic order for the transverse spins.

The spin model with reduced symmetry also has many gapless states characterized by the non-Lagrangian con-

densable algebra of the  $\mathcal{D}(D_8)$ -symTO. Those gapless states describe the critical points for the continuous phase transitions between the 11 gapped phases for the reduced symmetry. Similarly, after we restore the  $SO(3)$  symmetry, the gapless state of spin- $\frac{1}{2}$  Heisenberg chain also have many gapless neighboring states, describing the critical points for the continuous phase transitions between the above discussed gapped/gapless phases.

To summarize, the AF phase of spin- $\frac{1}{2}$  Heisenberg model (*i.e.* the commensurate gapless phase from condensable algebras  $\mathcal{A}_{2,2}, \mathcal{A}_{2,3}, \mathcal{A}_{2,4}$  with its classical picture Fig. 9) has the following neighboring phases or critical states:

1. A gapped commensurate dimer phase (from condensable algebra  $\mathcal{A}_{2,1}$ ). See Fig. 8.
2. A gapless commensurate ferromagnetic phase with  $\omega \sim k^2$  that breaks the translation symmetry (from condensable algebra  $\mathcal{A}_{3,1}, \mathcal{A}_{3,2}, \mathcal{A}_{3,3}$ ). See Fig. 10 for its classical picture.
3. A gapless translation symmetric incommensurate ferromagnetic phase with a linear mode  $\omega \sim |k|$ , and a quadratic mode  $\omega \sim k^2$  (from condensable algebra  $\mathcal{A}_{3,4}, \mathcal{A}_{3,5}, \mathcal{A}_{3,6}$ ). See Fig. 11 for its classical picture.
4. A gapless incommensurate ferromagnetic phase with a linear mode  $\omega \sim |k|$  and a quadratic mode  $\omega \sim k^2$ , as well as translation symmetry breaking (from condensable algebra  $\mathcal{A}_{1,1}$ ). See Fig. 12 for its classical picture.
5. Gapless states, describing the critical points for the stable or unstable continuous phase transitions between the above mentioned gapped/gapless phases. In general, the critical points between commensurate phases have a linear dispersion  $\omega \sim |k|$  and are commensurate states. The critical points between commensurate phases and incommensurate phases have a non-linear dispersion  $\omega \sim |k|^\gamma$ ,  $\gamma > 1$  and are commensurate states.

In this paper, the term “phase” denotes states whose properties remain robust under all symmetric perturbations. A stable continuous phase transition corresponds to a critical point with only one symmetric relevant operator. Conversely, an unstable continuous phase transition refers to a multi-critical point with two or more symmetric relevant operators.

We remark that the dimer phase (Fig. 8) and the anti-ferromagnetic phase (Fig. 9) are connected by the  $S_4$  automorphisms. Also, the ferromagnetic phase that breaks the translation symmetry (Fig. 10) and the ferromagnetic phase with anti-ferromagnetic order for transverse spin (Fig. 11) are connected by the  $S_4$  automorphisms. Those phases are also connected by the approximate emergent  $SO(4)$  symmetry, since the  $S_4$  automorphisms is a part of the  $SO(4)$  symmetry.

Since the  $S_3$  subgroup of the  $S_4$  automorphisms permute  $x, y, z$ , the  $S_3$  automorphisms is actually a part of  $SO(3)$  spin rotation symmetry. The three spectra in Fig. 5(b,c,d) are connected by the  $S_3$  automorphisms, and thus are identical due the  $SO(3)$  spin rotation symmetry. Similarly, the three spectra in Fig. 5(f,g,h) are identical since they are connected by the  $S_3$  automorphisms.

The spectrum in Fig. 5(e) and the three spectra in Fig. 5(f,g,h) are connected by the  $S_4$  automorphisms. From the ED calculation, we find that they are identical at low energies only. This indicates that the  $S_4$  automorphisms become low-energy emergent symmetries of the spin- $\frac{1}{2}$  Heisenberg chain.

We stress that for systems described by a symTO, the automorphisms of the symTO, in general, are not the symmetry of the systems. However, we can fine tune the systems to make the automorphisms to be the symmetry of fine-tuned systems. Also, if some of those systems are gapless, the automorphisms can be the emergent symmetry of those gapless systems. In our case, the gapless spin- $\frac{1}{2}$  Heisenberg chain has an emanant symmetry described by  $\mathcal{D}(D_8)$  symTO. Our numerical calculation suggests that the  $S_4$  automorphism of  $\mathcal{D}(D_8)$  symTO is an emergent symmetry of the gapless spin- $\frac{1}{2}$  Heisenberg chain.

## IX. CONCLUSION & OUTLOOK

We have shown that the  $SO(3)$ -symmetric Heisenberg chain has a low-energy emanant symmetry described by  $SO(3) \times \mathbb{Z}_2^t$  with a mixed anomaly. Can this emanant symmetry be captured holographically by a 2+1D symTO? Guided by the finite-group case, one might guess that the relevant symTO is simply a 2+1D  $SO(3) \times \mathbb{Z}_2^t$  gauge theory with a topological term specified by a cocycle in  $H^3(SO(3) \times \mathbb{Z}_2^t; \mathbb{R}/\mathbb{Z})$ :

$$e^{iS} = e^{i\pi \int_{M_{2+1}} w_2 \smile a + a \smile a \smile a}, \quad (47)$$

where  $a \in Z^1(M^{2+1}, \mathbb{Z}_2)$  is a 1-cocycle describing the flat connection of the  $\mathbb{Z}_2^t$  gauge field, and  $w_2 \in H^2(M^{2+1}, \mathbb{Z}_2)$  is the second Stiefel-Whitney class of the  $SO(3)$  bundle (equivalently the pullback of the universal class in  $H^2(BSO(3), \mathbb{Z}_2)$ ).

However, because  $SO(3)$  is a *continuous* group, the  $SO(3) \times \mathbb{Z}_2^t$  gauge theory is gapless in the flat-connection limit; it is not a topological field theory and therefore does not realize a topological order. From a purely categorical viewpoint, one might nevertheless attempt to define a twisted quantum double  $\mathcal{D}_{SO(3) \times \mathbb{Z}_2^t}^\omega$  (a braided tensor category) for the compact group  $SO(3) \times \mathbb{Z}_2^t$ , with  $\omega \in H^3(SO(3) \times \mathbb{Z}_2^t; \mathbb{R}/\mathbb{Z})$ . If an appropriate notion of *condensable algebra* can be formulated for  $\mathcal{D}_{SO(3) \times \mathbb{Z}_2^t}^\omega$ , then condensable algebras could be used to compute and classify the phases compatible with the emanant symTO  $\mathcal{D}_{SO(3) \times \mathbb{Z}_2^t}^\omega$ .

A pragmatic way to avoid continuous groups is to replace them by suitable *finite* subgroups of the continuous symmetry. This yields symTOs described by non-degenerate braided fusion categories in the trivial Witt class. After determining the phases via condensable algebras for these finite symTOs, one can then enlarge the symmetry and study how the phases evolve under symmetry enhancement. This is the route taken in this paper.

## ACKNOWLEDGMENTS

We thank Leon Balents and Christopher Mudry for insightful discussions. This research was supported in part by grant no. NSF PHY-2309135 to the Kavli Institute for Theoretical Physics (KITP). This work was partially supported by NSF grant DMR2022428 and by the Simons Collaboration on Ultra-Quantum Matter, which is a grant from the Simons Foundation (651446, XGW). ZJC acknowledges support from Kurt Forrester Foundation Fellowship. ÖMA is also supported by Swiss National Science Foundation (SNSF) under grant no. P500PT-214429.

**Appendix A:  $S$ -matrix and fusion rules of  $D_8$  quantum double  $\mathcal{D}(D_8)$**

The  $S$ -matrix of  $D_8$  quantum double is given by

$$S = \left( \begin{array}{c|c|c|c|c|c|c} \begin{array}{cccc} 1 & 1 & 1 & 1 \\ 1 & 1 & 1 & 1 \\ 1 & 1 & 1 & 1 \\ 1 & 1 & 1 & 1 \end{array} & \begin{array}{cccc} 1 & 1 & 1 & 1 \\ 1 & 1 & 1 & 1 \\ 1 & 1 & 1 & 1 \\ 1 & 1 & 1 & 1 \end{array} & \begin{array}{ccc} 2 & 2 & 2 \\ 2 & -2 & -2 \\ -2 & 2 & -2 \\ -2 & -2 & 2 \end{array} & \begin{array}{ccc} 2 & 2 & 2 \\ 2 & -2 & -2 \\ -2 & 2 & -2 \\ -2 & -2 & 2 \end{array} & \begin{array}{ccc} 2 & 2 & 2 \\ 2 & -2 & -2 \\ -2 & 2 & -2 \\ -2 & -2 & 2 \end{array} & \begin{array}{ccc} 2 & 2 & 2 \\ 2 & -2 & -2 \\ -2 & 2 & -2 \\ -2 & -2 & 2 \end{array} & \begin{array}{cc} 2 & 2 \\ 2 & 2 \\ 2 & 2 \\ 2 & 2 \end{array} \\ \hline \begin{array}{cccc} 1 & 1 & 1 & 1 \\ 1 & 1 & 1 & 1 \\ 1 & 1 & 1 & 1 \\ 1 & 1 & 1 & 1 \end{array} & \begin{array}{cccc} 1 & 1 & 1 & 1 \\ 1 & 1 & 1 & 1 \\ 1 & 1 & 1 & 1 \\ 1 & 1 & 1 & 1 \end{array} & \begin{array}{ccc} 2 & 2 & 2 \\ 2 & -2 & -2 \\ -2 & 2 & -2 \\ -2 & -2 & 2 \end{array} & \begin{array}{ccc} -2 & -2 & -2 \\ -2 & 2 & 2 \\ 2 & -2 & 2 \\ 2 & 2 & -2 \end{array} & \begin{array}{ccc} -2 & -2 & -2 \\ -2 & 2 & 2 \\ 2 & -2 & 2 \\ 2 & 2 & -2 \end{array} & \begin{array}{ccc} 2 & 2 & 2 \\ 2 & -2 & -2 \\ -2 & 2 & -2 \\ -2 & -2 & 2 \end{array} & \begin{array}{cc} -2 & -2 \\ -2 & -2 \\ -2 & -2 \\ -2 & -2 \end{array} \\ \hline \begin{array}{cccc} 2 & 2 & -2 & -2 \\ 2 & -2 & 2 & -2 \\ 2 & -2 & -2 & 2 \end{array} & \begin{array}{cccc} 2 & 2 & -2 & -2 \\ 2 & -2 & 2 & -2 \\ 2 & -2 & -2 & 2 \end{array} & \begin{array}{ccc} 4 & & \\ & 4 & \\ & & 4 \end{array} & & & \begin{array}{ccc} -4 & & \\ & -4 & \\ & & -4 \end{array} & \\ \hline \begin{array}{cccc} 2 & 2 & -2 & -2 \\ 2 & -2 & 2 & -2 \\ 2 & -2 & -2 & 2 \end{array} & \begin{array}{cccc} -2 & -2 & 2 & 2 \\ -2 & 2 & -2 & 2 \\ -2 & 2 & 2 & -2 \end{array} & & \begin{array}{ccc} 4 & & \\ & 4 & \\ & & 4 \end{array} & \begin{array}{ccc} -4 & & \\ & -4 & \\ & & -4 \end{array} & & \\ \hline \begin{array}{cccc} 2 & 2 & -2 & -2 \\ 2 & -2 & 2 & -2 \\ 2 & -2 & -2 & 2 \end{array} & \begin{array}{cccc} -2 & -2 & 2 & 2 \\ -2 & 2 & -2 & 2 \\ -2 & 2 & 2 & -2 \end{array} & & \begin{array}{ccc} -4 & & \\ & -4 & \\ & & -4 \end{array} & \begin{array}{ccc} 4 & & \\ & 4 & \\ & & 4 \end{array} & & \\ \hline \begin{array}{cccc} 2 & 2 & -2 & -2 \\ 2 & -2 & 2 & -2 \\ 2 & -2 & -2 & 2 \end{array} & \begin{array}{cccc} 2 & 2 & -2 & -2 \\ 2 & -2 & 2 & -2 \\ 2 & -2 & -2 & 2 \end{array} & \begin{array}{ccc} -4 & & \\ & -4 & \\ & & -4 \end{array} & & & \begin{array}{ccc} 4 & & \\ & 4 & \\ & & 4 \end{array} & \\ \hline \begin{array}{cccc} 2 & 2 & 2 & 2 \\ 2 & 2 & 2 & 2 \end{array} & \begin{array}{cccc} -2 & -2 & -2 & -2 \\ -2 & -2 & -2 & -2 \end{array} & & & & & \begin{array}{cc} -4 & 4 \\ 4 & -4 \end{array} \end{array} \right) \quad (A1)$$

The fusion rule is given by

$\otimes$	$\mathbb{1}$	$e_x$	$e_y$	$e_z$	$e_t$	$e_{xt}$	$e_{yt}$	$e_{zt}$	$m_x$	$m_y$	$m_z$	$m_{xt}$	$m_{yt}$	$m_{zt}$	$f_{xt}$	$f_{yt}$	$f_{zt}$	$f_x$	$f_y$	$f_z$	$s_t$	$s'_t$
$\mathbb{1}$	$\mathbb{1}$	$e_x$	$e_y$	$e_z$	$e_t$	$e_{xt}$	$e_{yt}$	$e_{zt}$	$m_x$	$m_y$	$m_z$	$m_{xt}$	$m_{yt}$	$m_{zt}$	$f_{xt}$	$f_{yt}$	$f_{zt}$	$f_x$	$f_y$	$f_z$	$s_t$	$s'_t$
$e_x$	$e_x$	$\mathbb{1}$	$e_z$	$e_y$	$e_{xt}$	$e_t$	$e_{zt}$	$e_{yt}$	$m_x$	$f_y$	$f_z$	$m_{xt}$	$f_{yt}$	$f_{zt}$	$f_{xt}$	$m_{yt}$	$m_{zt}$	$f_x$	$m_y$	$m_z$	$s_t$	$s'_t$
$e_y$	$e_y$	$e_z$	$\mathbb{1}$	$e_x$	$e_{yt}$	$e_{zt}$	$e_t$	$e_{xt}$	$f_x$	$m_y$	$f_z$	$f_{xt}$	$m_{yt}$	$f_{zt}$	$m_{xt}$	$f_{yt}$	$m_{zt}$	$m_x$	$f_y$	$m_z$	$s_t$	$s'_t$
$e_z$	$e_z$	$e_y$	$e_x$	$\mathbb{1}$	$e_{zt}$	$e_{yt}$	$e_{xt}$	$e_t$	$f_x$	$f_y$	$m_z$	$f_{xt}$	$f_{yt}$	$m_{zt}$	$m_{xt}$	$m_{yt}$	$f_{zt}$	$m_x$	$m_y$	$f_z$	$s_t$	$s'_t$
$e_t$	$e_t$	$e_{xt}$	$e_{yt}$	$e_{zt}$	$\mathbb{1}$	$e_x$	$e_y$	$e_z$	$m_x$	$m_y$	$m_z$	$f_{xt}$	$f_{yt}$	$f_{zt}$	$m_{xt}$	$m_{yt}$	$m_{zt}$	$f_x$	$f_y$	$f_z$	$s'_t$	$s_t$
$e_{xt}$	$e_{xt}$	$e_t$	$e_{zt}$	$e_{yt}$	$e_x$	$\mathbb{1}$	$e_z$	$e_y$	$f_x$	$f_y$	$f_z$	$m_{xt}$	$m_{yt}$	$m_{zt}$	$f_{xt}$	$m_{yt}$	$m_{zt}$	$f_x$	$m_y$	$m_z$	$s'_t$	$s_t$
$e_{yt}$	$e_{yt}$	$e_{zt}$	$e_t$	$e_{xt}$	$e_y$	$e_z$	$\mathbb{1}$	$e_x$	$f_x$	$m_y$	$f_z$	$m_{xt}$	$f_{yt}$	$m_{zt}$	$f_{xt}$	$m_{yt}$	$m_{zt}$	$m_x$	$f_y$	$m_z$	$s'_t$	$s_t$
$e_{zt}$	$e_{zt}$	$e_{yt}$	$e_{xt}$	$e_t$	$e_z$	$e_y$	$e_x$	$\mathbb{1}$	$f_x$	$f_y$	$m_z$	$m_{xt}$	$m_{yt}$	$f_{zt}$	$f_{xt}$	$m_{yt}$	$m_{zt}$	$m_x$	$m_y$	$f_z$	$s'_t$	$s_t$
$m_x$	$m_x$	$m_x$	$f_x$	$f_x$	$m_x$	$m_x$	$f_x$	$f_x$	$\mathbb{1} \oplus e_x \oplus e_t \oplus e_{xt}$	$m_z \oplus f_z$	$m_y \oplus f_y$	$s_t \oplus s'_t$	$m_{zt} \oplus f_{zt}$	$m_{yt} \oplus f_{yt}$	$s_t \oplus s'_t$	$m_z \oplus e_z \oplus e_{yt} \oplus e_{zt}$	$m_x \oplus f_z$	$m_y \oplus e_y \oplus e_{xt} \oplus e_{zt}$	$m_z \oplus f_z$	$m_x \oplus f_y$	$m_{xt} \oplus f_{xt}$	$m_{zt} \oplus f_{zt}$
$m_y$	$m_y$	$f_y$	$m_y$	$f_y$	$m_y$	$f_y$	$m_y$	$f_y$	$m_z \oplus f_z$	$\mathbb{1} \oplus e_y \oplus e_t \oplus e_{yt}$	$m_x \oplus f_x$	$m_{zt} \oplus f_{zt}$	$s_t \oplus s'_t$	$m_{xt} \oplus f_{xt}$	$m_{yt} \oplus f_{yt}$	$m_z \oplus f_z$	$m_x \oplus f_y$	$m_y \oplus e_y \oplus e_{xt} \oplus e_{zt}$	$m_z \oplus f_z$	$m_x \oplus f_y$	$m_{yt} \oplus f_{yt}$	$m_{zt} \oplus f_{zt}$
$m_z$	$m_z$	$f_z$	$f_z$	$m_z$	$m_z$	$f_z$	$f_z$	$m_z$	$m_y \oplus f_y$	$m_x \oplus f_x$	$\mathbb{1} \oplus e_z \oplus e_t \oplus e_{zt}$	$m_{yt} \oplus f_{yt}$	$m_{xt} \oplus f_{xt}$	$s_t \oplus s'_t$	$m_y \oplus f_y$	$e_x \oplus e_y \oplus e_{xt} \oplus e_{zt}$	$m_x \oplus f_z$	$m_y \oplus f_y$	$m_z \oplus f_z$	$e_x \oplus e_y \oplus e_{xt} \oplus e_{zt}$	$m_{zt} \oplus f_{zt}$	$m_{yt} \oplus f_{yt}$
$m_{xt}$	$m_{xt}$	$m_{xt}$	$f_{xt}$	$f_{xt}$	$f_{xt}$	$m_{xt}$	$m_{xt}$	$m_{xt}$	$s_t \oplus s'_t$	$m_{zt} \oplus f_{zt}$	$\mathbb{1} \oplus e_x \oplus e_{yt} \oplus e_{zt}$	$m_y \oplus f_y$	$m_z \oplus f_z$	$m_{xt} \oplus f_{xt}$	$e_y \oplus e_z \oplus e_t \oplus e_{xt}$	$m_x \oplus f_z$	$m_y \oplus f_y$	$s_t \oplus s'_t$	$m_z \oplus f_z$	$m_{xt} \oplus f_{xt}$	$m_x \oplus f_y$	$m_{yt} \oplus f_{yt}$
$m_{yt}$	$m_{yt}$	$f_{yt}$	$m_{yt}$	$f_{yt}$	$m_{yt}$	$f_{yt}$	$m_{yt}$	$f_{yt}$	$m_{zt} \oplus f_{zt}$	$\mathbb{1} \oplus e_y \oplus e_t \oplus e_{yt}$	$m_x \oplus f_x$	$m_{zt} \oplus f_{zt}$	$s_t \oplus s'_t$	$m_{xt} \oplus f_{xt}$	$e_y \oplus e_z \oplus e_t \oplus e_{xt}$	$m_x \oplus f_z$	$m_y \oplus f_y$	$m_z \oplus f_z$	$m_{xt} \oplus f_{xt}$	$m_x \oplus f_y$	$m_{yt} \oplus f_{yt}$	$m_{zt} \oplus f_{zt}$
$m_{zt}$	$m_{zt}$	$f_{zt}$	$m_{zt}$	$f_{zt}$	$m_{zt}$	$f_{zt}$	$m_{zt}$	$f_{zt}$	$m_{xt} \oplus f_{xt}$	$s_t \oplus s'_t$	$m_y \oplus f_y$	$m_z \oplus f_z$	$m_{xt} \oplus f_{xt}$	$\mathbb{1} \oplus e_z \oplus e_{xt} \oplus e_{zt}$	$m_y \oplus f_y$	$m_x \oplus f_z$	$m_y \oplus f_y$	$m_z \oplus f_z$	$m_{xt} \oplus f_{xt}$	$m_x \oplus f_z$	$m_y \oplus f_y$	$m_{zt} \oplus f_{zt}$
$f_{xt}$	$f_{xt}$	$m_{xt}$	$m_{xt}$	$m_{xt}$	$m_{xt}$	$f_{xt}$	$m_{xt}$	$f_{xt}$	$s_t \oplus s'_t$	$m_{zt} \oplus f_{zt}$	$m_y \oplus f_y$	$m_z \oplus f_z$	$m_{xt} \oplus f_{xt}$	$\mathbb{1} \oplus e_x \oplus e_{yt} \oplus e_{zt}$	$m_y \oplus f_y$	$m_x \oplus f_z$	$m_y \oplus f_y$	$m_z \oplus f_z$	$m_{xt} \oplus f_{xt}$	$m_x \oplus f_z$	$m_y \oplus f_y$	$m_{zt} \oplus f_{zt}$
$f_{yt}$	$f_{yt}$	$m_{yt}$	$m_{yt}$	$m_{yt}$	$f_{yt}$	$m_{yt}$	$f_{yt}$	$f_{yt}$	$m_{zt} \oplus f_{zt}$	$s_t \oplus s'_t$	$m_x \oplus f_x$	$m_z \oplus f_z$	$m_{xt} \oplus f_{xt}$	$\mathbb{1} \oplus e_y \oplus e_{xt} \oplus e_{zt}$	$m_y \oplus f_y$	$m_x \oplus f_z$	$m_y \oplus f_y$	$m_z \oplus f_z$	$m_{xt} \oplus f_{xt}$	$m_x \oplus f_z$	$m_y \oplus f_y$	$m_{zt} \oplus f_{zt}$
$f_{zt}$	$f_{zt}$	$m_{zt}$	$m_{zt}$	$f_{zt}$	$m_{zt}$	$f_{zt}$	$m_{zt}$	$f_{zt}$	$m_{yt} \oplus f_{yt}$	$m_{xt} \oplus f_{xt}$	$s_t \oplus s'_t$	$m_y \oplus f_y$	$m_z \oplus f_z$	$m_{xt} \oplus f_{xt}$	$\mathbb{1} \oplus e_z \oplus e_{xt} \oplus e_{zt}$	$m_y \oplus f_y$	$m_x \oplus f_z$	$m_y \oplus f_y$	$m_z \oplus f_z$	$m_{xt} \oplus f_{xt}$	$m_x \oplus f_z$	$m_y \oplus f_y$
$f_x$	$f_x$	$m_x$	$m_x$	$m_x$	$f_x$	$f_x$	$m_x$	$m_x$	$e_y \oplus e_z \oplus e_{yt} \oplus e_{zt}$	$m_z \oplus f_z$	$m_y \oplus f_y$	$s_t \oplus s'_t$	$m_{zt} \oplus f_{zt}$	$m_{yt} \oplus f_{yt}$	$s_t \oplus s'_t$	$\mathbb{1} \oplus e_x \oplus e_{xt} \oplus e_{zt}$	$m_z \oplus f_z$	$m_y \oplus f_y$	$m_z \oplus f_z$	$m_{xt} \oplus f_{xt}$	$m_{xt} \oplus f_{xt}$	$m_{zt} \oplus f_{zt}$
$f_y$	$f_y$	$m_y$	$f_y$	$m_y$	$f_y$	$m_y$	$f_y$	$m_y$	$m_z \oplus f_z$	$e_x \oplus e_z \oplus e_{xt} \oplus e_{zt}$	$m_x \oplus f_x$	$m_{zt} \oplus f_{zt}$	$s_t \oplus s'_t$	$m_{xt} \oplus f_{xt}$	$m_{yt} \oplus f_{yt}$	$\mathbb{1} \oplus e_y \oplus e_t \oplus e_{yt}$	$m_x \oplus f_z$	$\mathbb{1} \oplus e_y \oplus e_t \oplus e_{yt}$	$m_x \oplus f_z$	$m_{yt} \oplus f_{yt}$	$m_{yt} \oplus f_{yt}$	$m_{zt} \oplus f_{zt}$
$f_z$	$f_z$	$m_z$	$m_z$	$f_z$	$m_z$	$f_z$	$m_z$	$f_z$	$m_y \oplus f_y$	$m_x \oplus f_x$	$e_x \oplus e_y \oplus e_{xt} \oplus e_{zt}$	$m_z \oplus f_z$	$m_{xt} \oplus f_{xt}$	$s_t \oplus s'_t$	$m_y \oplus f_y$	$m_x \oplus f_z$	$\mathbb{1} \oplus e_z \oplus e_t \oplus e_{zt}$	$m_y \oplus f_y$	$m_x \oplus f_z$	$\mathbb{1} \oplus e_z \oplus e_t \oplus e_{zt}$	$m_{zt} \oplus f_{zt}$	$m_{zt} \oplus f_{zt}$
$s_t$	$s_t$	$s_t$	$s_t$	$s_t$	$s'_t$	$s'_t$	$s'_t$	$s'_t$	$m_{xt} \oplus f_{xt}$	$m_{yt} \oplus f_{yt}$	$m_z \oplus f_z$	$m_x \oplus f_x$	$m_y \oplus f_y$	$m_z \oplus f_z$	$m_{xt} \oplus f_{xt}$	$m_{yt} \oplus f_{yt}$	$m_z \oplus f_z$	$m_{xt} \oplus f_{xt}$	$m_{yt} \oplus f_{yt}$	$m_z \oplus f_z$	$\mathbb{1} \oplus e_x \oplus e_y \oplus e_z$	$e_t \oplus e_{xt} \oplus e_{zt}$
$s'_t$	$s'_t$	$s'_t$	$s'_t$	$s'_t$	$s_t$	$s_t$	$s_t$	$s_t$	$m_{xt} \oplus f_{xt}$	$m_{yt} \oplus f_{yt}$	$m_z \oplus f_z$	$m_x \oplus f_x$	$m_y \oplus f_y$	$m_z \oplus f_z$	$m_{xt} \oplus f_{xt}$	$m_{yt} \oplus f_{yt}$	$m_z \oplus f_z$	$m_{xt} \oplus f_{xt}$	$m_{yt} \oplus f_{yt}$	$m_z \oplus f_z$	$e_t \oplus e_{xt} \oplus e_{zt}$	$\mathbb{1} \oplus e_x \oplus e_y \oplus e_z$



- 
- [1] M. Cheng and N. Seiberg, Lieb-Schultz-Mattis, Luttinger, and 't Hooft - anomaly matching in lattice systems, *SciPost Physics* **15**, 051 (2023), [arXiv:2211.12543](#).
- [2] M. A. Metlitski and R. Thorngren, Intrinsic and emergent anomalies at deconfined critical points, *Phys. Rev. B* **98**, 085140 (2018), [arXiv:1707.07686](#).
- [3] X.-G. Wen, Emergent (anomalous) higher symmetries from topological order and from dynamical electromagnetic field in condensed matter systems, *Phys. Rev. B* **99**, 205139 (2019), [arXiv:1812.02517](#).
- [4] M. Barkeshli, C. Feuchis, Z. Komargodski, and S. Zhong, Disclinations, dislocations, and emanant flux at Dirac criticality, [arXiv:2501.13866 \[cond-mat.str-el\]](#) (2025), [arXiv:2501.13866](#).
- [5] Z. Nussinov and G. Ortiz, Sufficient symmetry conditions for topological quantum order, *Proc. Natl. Acad. Sci. U.S.A.* **106**, 16944 (2009), [arXiv:cond-mat/0605316](#).
- [6] Z. Nussinov and G. Ortiz, A symmetry principle for topological quantum order, *Ann. Phys.* **324**, 977 (2009), [arXiv:cond-mat/0702377](#).
- [7] A. Kapustin and R. Thorngren, Higher Symmetry and Gapped Phases of Gauge Theories, in *Algebra, Geometry, and Physics in the 21st Century: Kontsevich Festschrift*, edited by D. Auroux, L. Katzarkov, T. Pantev, Y. Soibelman, and Y. Tschinkel (Birkhäuser, Cham, 2017) pp. 177–202, [arXiv:1309.4721](#).
- [8] D. Gaiotto, A. Kapustin, N. Seiberg, and B. Willett, Generalized global symmetries, *J. High Energ. Phys.* **2015** (2), 172, [arXiv:1412.5148](#).
- [9] G. 't Hooft, Naturalness, chiral symmetry, and spontaneous chiral symmetry breaking, in *Recent Developments in Gauge Theories. NATO Advanced Study Institutes Series (Series B. Physics)*, Vol. 59, edited by G. 't Hooft et al. (Springer, Boston, MA., 1980) pp. 135–157.
- [10] X. Chen, Z.-C. Gu, Z.-X. Liu, and X.-G. Wen, Symmetry protected topological orders and the group cohomology of their symmetry group, *Phys. Rev. B* **87**, 155114 (2013), [arXiv:1106.4772](#).
- [11] X.-G. Wen, Classifying gauge anomalies through symmetry-protected trivial orders and classifying gravitational anomalies through topological orders, *Phys. Rev. D* **88**, 045013 (2013), [arXiv:1303.1803](#).
- [12] A. Kapustin and R. Thorngren, Anomalous discrete symmetries in three dimensions and group cohomology, *Physical Review Letter* **112**, 231602 (2014), [arXiv:1403.0617](#).
- [13] C. Wang, A. Nahum, M. A. Metlitski, C. Xu, and T. Senthil, Deconfined Quantum Critical Points: Symmetries and Dualities, *Phys. Rev. X* **7**, 031051 (2017), [arXiv:1703.02426](#).
- [14] R. Thorngren and C. von Keyserlingk, Higher SPT's and a generalization of anomaly in-flow (2015), [arXiv:1511.02929](#).
- [15] Y. Tachikawa, On gauging finite subgroups, *SciPost Phys.* **8**, 015 (2020), [arXiv:1712.09542](#).
- [16] A. J. Parzygnat, Two-dimensional algebra in lattice gauge theory, *J. Math. Phys.* **60**, 043506 (2019), [arXiv:1802.01139](#).
- [17] C. Delcamp and A. Tiwari, From gauge to higher gauge models of topological phases, *J. High Energ. Phys.* **2018** (10), 49, [arXiv:1802.10104](#).
- [18] F. Benini, C. Córdova, and P.-S. Hsin, On 2-group global symmetries and their anomalies, *J. High Energ. Phys.* **2019** (3), 118, [arXiv:1803.09336](#).
- [19] C. Zhu, T. Lan, and X.-G. Wen, Topological nonlinear  $\sigma$ -model, higher gauge theory, and a systematic construction of 3+1D topological orders for boson systems, *Phys. Rev. B* **100**, 045105 (2019), [arXiv:1808.09394](#).
- [20] Z. Wan, J. Wang, and Y. Zheng, New Higher Anomalies, SU(N) Yang-Mills Gauge Theory and  $\mathbb{CP}^{N-1}$  Sigma Model, *Annals of Physics* **414**, 168074 (2020), [arXiv:1812.11968](#).
- [21] Z. Wan and J. Wang, Higher anomalies, higher symmetries, and cobordisms I: classification of higher-symmetry-protected topological states and their boundary fermionic/bosonic anomalies via a generalized cobordism theory, *Annals of Mathematical Sciences and Applications* **4**, 107 (2019), [arXiv:1812.11967](#).
- [22] M. Guo, K. Ohmori, P. Putrov, Z. Wan, and J. Wang, Fermionic Finite-Group Gauge Theories and Interacting Symmetric/Crystalline Orders via Cobordisms, *Communications in Mathematical Physics* **376**, 1073 (2020), [arXiv:1812.11959](#).
- [23] Z. Wan and J. Wang, Adjoint QCD4, deconfined critical phenomena, symmetry-enriched topological quantum field theory, and higher symmetry extension, *Phys. Rev. D* **99**, 065013 (2019), [arXiv:1812.11955](#).
- [24] V. B. Petkova and J. B. Zuber, Generalised twisted partition functions, *Physics Letters B* **504**, 157 (2001), [arXiv:hep-th/0011021](#).
- [25] R. Coquereaux and G. Schieber, Twisted partition functions for ADE boundary conformal field theories and Ocneanu algebras of quantum symmetries, *Journal of Geometry and Physics* **42**, 216 (2002), [arXiv:hep-th/0107001](#).
- [26] J. Fuchs, I. Runkel, and C. Schweigert, TFT construction of RCFT correlators I: partition functions, *Nuclear Physics B* **646**, 353 (2002), [arXiv:hep-th/0204148](#).
- [27] J. Fröhlich, J. Fuchs, I. Runkel, and C. Schweigert, Duality and defects in rational conformal field theory, *Nucl. Phys. B* **763**, 354 (2007), [arXiv:hep-th/0607247](#).
- [28] J. Fröhlich, J. Fuchs, I. Runkel, and C. Schweigert, Defect Lines, Dualities and Generalised Orbifolds, in *XVTH INTERNATIONAL CONGRESS ON MATHEMATICAL PHYSICS. Held 3-8 August 2009 in Prague* (World Scientific, Singapore, 2010) pp. 608–613, [arXiv:0909.5013](#).
- [29] A. Davydov, L. Kong, and I. Runkel, Field theories with defects and the centre functor, *Proceedings of Symposia in Pure Mathematics* **83**, 71 (2011), [arXiv:1107.0495](#).
- [30] L. Bhardwaj and Y. Tachikawa, On finite symmetries and their gauging in two dimensions, *J. High Energ. Phys.* **2018** (3), 189, [arXiv:1704.02330](#).
- [31] C.-M. Chang, Y.-H. Lin, S.-H. Shao, Y. Wang, and X. Yin, Topological defect lines and renormalization group flows in two dimensions, *J. High Energ. Phys.* **2019** (1), 26, [arXiv:1802.04445](#).
- [32] R. Thorngren and Y. Wang, Fusion Category Symmetry I: Anomaly In-Flow and Gapped Phases, *J. High Energ. Phys.* **2024**, 132, [arXiv:1912.02817](#).

- [33] L. Kong, W. Yuan, and H. Zheng, Pointed Drinfeld Center Functor, *Communications in Mathematical Physics* **381**, 1409 (2021), [arXiv:1912.13168](#).
- [34] K. Inamura, Topological field theories and symmetry protected topological phases with fusion category symmetries, *Journal of High Energy Physics* **2021**, 204 (2021), [arXiv:2103.15588](#).
- [35] T. Quella, Symmetry-protected topological phases beyond groups: The q-deformed Affleck-Kennedy-Lieb-Tasaki model, *Physical Review B* **102**, 081120 (2020), [arXiv:2005.09072](#).
- [36] L. Kong, T. Lan, X.-G. Wen, Z.-H. Zhang, and H. Zheng, Classification of topological phases with finite internal symmetries in all dimensions, *J. High Energ. Phys.* **2020** (9), 93, [arXiv:2003.08898](#).
- [37] L. Kong, T. Lan, X.-G. Wen, Z.-H. Zhang, and H. Zheng, Algebraic higher symmetry and categorical symmetry: A holographic and entanglement view of symmetry, *Phys. Rev. Res.* **2**, 043086 (2020), [arXiv:2005.14178](#).
- [38] B. Heidenreich, J. McNamara, M. Montero, M. Reece, T. Rudelius, and I. Valenzuela, Chern-Weil global symmetries and how quantum gravity avoids them, *Journal of High Energy Physics* **2021**, 53 (2021), [arXiv:2012.00009](#).
- [39] J. Kaidi, K. Ohmori, and Y. Zheng, Kramers-Wannier-like Duality Defects in  $(3+1)$ D Gauge Theories, *Physical Review Letter* **128**, 111601 (2022), [arXiv:2111.01141](#).
- [40] Y. Choi, C. Córdova, P.-S. Hsin, H. T. Lam, and S.-H. Shao, Noninvertible duality defects in  $3+1$  dimensions, *Phys. Rev. D* **105**, 125016 (2022), [arXiv:2111.01139](#).
- [41] L. Bhardwaj, L. E. Bottini, S. Schäfer-Nameki, and A. Tiwari, Non-invertible higher-categorical symmetries, *SciPost Physics* **14**, 007 (2023), [arXiv:2204.06564](#).
- [42] D. S. Freed, G. W. Moore, and C. Teleman, Topological symmetry in quantum field theory (2022), [arXiv:2209.07471](#).
- [43] L. Kong and X.-G. Wen, Braided fusion categories, gravitational anomalies, and the mathematical framework for topological orders in any dimensions, (2014), [arXiv:1405.5858](#).
- [44] D. Fiorenza and A. Valentino, Boundary conditions for topological quantum field theories, anomalies and projective modular functors, *Commun. Math. Phys.* **338**, 1043 (2015), [arXiv:1409.5723](#).
- [45] S. Monnier, Hamiltonian anomalies from extended field theories, *Commun. Math. Phys.* **338**, 1327 (2015), [arXiv:1410.7442](#).
- [46] L. Kong, X.-G. Wen, and H. Zheng, Boundary-bulk relation for topological orders as the functor mapping higher categories to their centers (2015), [arXiv:1502.01690](#).
- [47] L. Kong, X.-G. Wen, and H. Zheng, Boundary-bulk relation in topological orders, *Nucl. Phys. B* **922**, 62 (2017), [arXiv:1702.00673](#).
- [48] W. Ji and X.-G. Wen, Non-invertible anomalies and mapping-class-group transformation of anomalous partition functions, *Phys. Rev. Research* **1**, 033054 (2019), [arXiv:1905.13279](#).
- [49] W. Ji and X.-G. Wen, Categorical symmetry and non-invertible anomaly in symmetry-breaking and topological phase transitions, *Phys. Rev. Res.* **2**, 033417 (2020), [arXiv:1912.13492](#).
- [50] M. Levin and X.-G. Wen, Detecting topological order in a ground state wave function, *Phys. Rev. Lett.* **96**, 110405 (2006), [arXiv:cond-mat/0510613](#).
- [51] S. Yang, L. Lehman, D. Poilblanc, K. Van Acoleyen, F. Verstraete, J. I. Cirac, and N. Schuch, Edge theories in projected entangled pair state models, *Physical Review Letter* **112**, 036402 (2014), [arXiv:1309.4596](#).
- [52] L. Kong and H. Zheng, Gapless edges of 2d topological orders and enriched monoidal categories, *Nucl. Phys. B* **927**, 140 (2018), [arXiv:1705.01087](#).
- [53] D. S. Freed and C. Teleman, Topological dualities in the Ising model, *Geom. Topol.* **26**, 1907 (2022), [arXiv:1806.00008](#).
- [54] J. Pulmann, P. Severa, and F. Valach, A non-abelian duality for (higher) gauge theories, *arXiv e-prints* **10.48550/arXiv.1909.06151** (2019), [arXiv:1909.06151](#).
- [55] T. Lichtman, R. Thorngren, N. H. Lindner, A. Stern, and E. Berg, Bulk anyons as edge symmetries: Boundary phase diagrams of topologically ordered states, *Physical Review B* **104**, 075141 (2021), [arXiv:2003.04328](#).
- [56] L. Kong and H. Zheng, A mathematical theory of gapless edges of 2d topological orders I, *J. High Energ. Phys.* **2020**, 150, [arXiv:1905.04924](#).
- [57] D. Gaiotto and J. Kulp, Orbifold groupoids, *J. High Energ. Phys.* **2021** (2), 132, [arXiv:2008.05960](#).
- [58] F. Apruzzi, F. Bonetti, I. G. Etzebarria, S. S. Hosseini, and S. Schäfer-Nameki, Symmetry TFTs from string theory, *Communications in Mathematical Physics* **402**, 895 (2023), [arXiv:2112.02092 \[hep-th\]](#).
- [59] A. Chatterjee and X.-G. Wen, Holographic theory for continuous phase transitions: Emergence and symmetry protection of gaplessness, *Phys. Rev. B* **108**, 075105 (2023), [arXiv:2205.06244](#).
- [60] H. Moradi, S. Farough Moosavian, and A. Tiwari, Topological holography: Towards a unification of Landau and beyond-Landau physics, *SciPost Phys. Core* **6**, 066 (2023), [arXiv:2207.10712](#).
- [61] A. Chatterjee, W. Ji, and X.-G. Wen, Emergent generalized symmetry and maximal symmetry-topological-order (2022), [arXiv:2212.14432](#).
- [62] R. Wen and A. C. Potter, Classification of  $1+1$ d gapless symmetry protected phases via topological holography (2023), [arXiv:2311.00050](#).
- [63] L. Bhardwaj, L. E. Bottini, D. Pajer, and S. Schäfer-Nameki, The Club Sandwich: Gapless Phases and Phase Transitions with Non-Invertible Symmetries, *SciPost Phys.* **18**, 156 (2025), [arXiv:2312.17322 \[hep-th\]](#).
- [64] L. Bhardwaj, D. Pajer, S. Schafer-Nameki, and A. Warman, Hasse Diagrams for Gapless SPT and SSB Phases with Non-Invertible Symmetries **10.48550/arXiv.2403.00905** (2024), [arXiv:2403.00905](#).
- [65] A. Chatterjee, Ö. M. Aksoy, and X.-G. Wen, Quantum phases and transitions in spin chains with non-invertible symmetries, *SciPost Physics* **17**, 115 (2024), [arXiv:2405.05331 \[cond-mat.str-el\]](#).
- [66] L. Bhardwaj, K. Inamura, and A. Tiwari, Fermionic non-invertible symmetries in  $(1+1)$ d: Gapped and gapless phases, transitions, and symmetry TFTs, *SciPost Physics* **18**, 194 (2025), [arXiv:2405.09754 \[hep-th\]](#).
- [67] L. Bhardwaj, L. E. Bottini, S. Schäfer-Nameki, and A. Tiwari, Illustrating the categorical Landau paradigm in lattice models, *Phys. Rev. B* **111**, 054432 (2025), [arXiv:2405.05302 \[cond-mat.str-el\]](#).

- [68] D.-C. Lu, Z. Sun, and Z. Zhang, Exploring  $G$ -ality defects in 2-dim QFTs [10.48550/arXiv.2406.12151](#) (2024), [arXiv:2406.12151](#).
- [69] R. Wen, String condensation and topological holography for 2+1D gapless SPT, [arXiv e-prints](#), [arXiv:2408.05801](#) (2024), [arXiv:2408.05801 \[cond-mat.str-el\]](#).
- [70] L. Bhardwaj, D. Pajer, S. Schafer-Nameki, A. Tiwari, A. Warman, and J. Wu, Gapped Phases in (2+1)d with Non-Invertible Symmetries: Part I, (2024), [arXiv:2408.05266 \[hep-th\]](#).
- [71] A. Antinucci, C. Copetti, and S. Schäfer-Nameki, SymTFT for (3+1)d Gapless SPTs and Obstructions to Confinement, *SciPost Phys.* **18**, 114 (2025), [arXiv:2408.05585 \[hep-th\]](#).
- [72] L. Bhardwaj, C. Copetti, D. Pajer, and S. Schafer-Nameki, Boundary SymTFT, [arXiv e-prints](#), [arXiv:2409.02166](#) (2024), [arXiv:2409.02166 \[hep-th\]](#).
- [73] S. D. Pace, H. T. Lam, and Ö. M. Aksoy, (SPT-)LSM theorems from projective non-invertible symmetries, *SciPost Physics* **18**, 028 (2025), [arXiv:2409.18113 \[cond-mat.str-el\]](#).
- [74] L. Bhardwaj, S. Schäfer-Nameki, A. Tiwari, and A. Warman, Gapped Phases in (2+1)d with Non-Invertible Symmetries: Part II, (2025), [arXiv:2502.20440 \[hep-th\]](#).
- [75] L. Bhardwaj, Y. Gai, S.-J. Huang, K. Inamura, S. Schafer-Nameki, A. Tiwari, and A. Warman, Gapless Phases in (2+1)d with Non-Invertible Symmetries, (2025), [arXiv:2503.12699](#).
- [76] Ö. M. Aksoy and X.-G. Wen, Phases with non-invertible symmetries in 1+1D – symmetry protected topological orders as duality automorphisms, [arXiv e-prints](#) [10.48550/arXiv.2503.21764](#) (2025), [arXiv:2503.21764](#).
- [77] R. Wen, Topological Holography for 2+1-D Gapped and Gapless Phases with Generalized Symmetries, [arXiv e-prints](#), [arXiv:2503.13685](#) (2025), [arXiv:2503.13685 \[hep-th\]](#).
- [78] S. D. Pace, Ö. M. Aksoy, and H. T. Lam, Space-time symmetry-enriched SymTFT: from LSM anomalies to modulated symmetries and beyond, [arXiv e-prints](#), [arXiv:2507.02036](#) (2025), [arXiv:2507.02036 \[cond-mat.str-el\]](#).
- [79] S. Schafer-Nameki, A. Tiwari, A. Warman, and C. Zhang, SymTFT Approach for Mixed States with Non-Invertible Symmetries, [arXiv e-prints](#), [arXiv:2507.05350](#) (2025), [arXiv:2507.05350 \[quant-ph\]](#).
- [80] I. Affleck and F. D. M. Haldane, Critical theory of quantum spin chains, *Phys. Rev. B* **36**, 5291 (1987).
- [81] P. Patil, E. Katz, and A. W. Sandvik, Numerical investigations of  $so(4)$  emergent extended symmetry in spin- $\frac{1}{2}$  heisenberg antiferromagnetic chains, *Phys. Rev. B* **98**, 014414 (2018).
- [82] E. Lieb, T. Schultz, and D. Mattis, Two soluble models of an antiferromagnetic chain, *Annals of Physics* **16**, 407 (1961).
- [83] M. Oshikawa, Commensurability, excitation gap, and topology in quantum many-particle systems on a periodic lattice, *Phys. Rev. Lett.* **84**, 1535 (2000).
- [84] Y. Ogata and H. Tasaki, Lieb-Schultz-Mattis Type Theorems for Quantum Spin Chains Without Continuous Symmetry, *Communications in Mathematical Physics* **372**, 951 (2019), [arXiv:1808.08740 \[math-ph\]](#).
- [85] Y. Ogata, Y. Tachikawa, and H. Tasaki, General Lieb-Schultz-Mattis Type Theorems for Quantum Spin Chains, *Communications in Mathematical Physics* **385**, 79 (2021), [arXiv:2004.06458 \[math-ph\]](#).
- [86] Y. Yao and M. Oshikawa, Twisted Boundary Condition and Lieb-Schultz-Mattis Inapplicability for Discrete Symmetries, *Phys. Rev. Lett.* **126**, 217201 (2021), [arXiv:2010.09244 \[cond-mat.str-el\]](#).
- [87] G. Y. Cho, C.-T. Hsieh, and S. Ryu, Anomaly manifestation of Lieb-Schultz-Mattis theorem and topological phases, *Phys. Rev. B* **96**, 195105 (2017), [arXiv:1705.03892 \[cond-mat.str-el\]](#).
- [88] Ö. M. Aksoy, C. Mudry, A. Furusaki, and A. Tiwari, Lieb-Schultz-Mattis anomalies and web of dualities induced by gauging in quantum spin chains, *SciPost Physics* **16**, 022 (2024), [arXiv:2308.00743 \[cond-mat.str-el\]](#).
- [89] S. Seifnashri, Lieb-schultz-mattis anomalies as obstructions to gauging (non-on-site) symmetries, *SciPost Physics* **16**, 10.21468/scipostphys.16.4.098 (2024).
- [90] S. Eggert, Numerical evidence for multiplicative logarithmic corrections from marginal operators, *Phys. Rev. B* **54**, R9612 (1996).
- [91] K. Okamoto and K. Nomura, Fluid-dimer critical point in  $s = 12$  antiferromagnetic heisenberg chain with next nearest neighbor interactions, *Physics Letters A* **169**, 433 (1992).
- [92] I. Affleck, Quantum spin chains and the haldane gap, *Journal of Physics: Condensed Matter* **1**, 3047 (1989).
- [93] A. Nersisyan, A. Luther, and F. Kusmartsev, Scaling properties of the two-chain model, *Physics Letters A* **176**, 363 (1993).
- [94] C. Mudry, A. Furusaki, T. Morimoto, and T. Hikihara, Quantum phase transitions beyond landau-ginzburg theory in one-dimensional space revisited, *Physical Review B* **99**, 10.1103/physrevb.99.205153 (2019).
- [95] W. Ji and X.-G. Wen, A unified view on symmetry, anomalous symmetry and non-invertible gravitational anomaly (2021), [arXiv:2106.02069](#).
- [96] N. Seiberg and S.-H. Shao, Majorana chain and Ising model - (non-invertible) translations, anomalies, and emanant symmetries, *SciPost Physics* **16**, 064 (2024), [arXiv:2307.02534 \[cond-mat.str-el\]](#).
- [97] N. Seiberg, S. Seifnashri, and S.-H. Shao, Non-invertible symmetries and LSM-type constraints on a tensor product Hilbert space, *SciPost Physics* **16**, 154 (2024), [arXiv:2401.12281 \[cond-mat.str-el\]](#).
- [98] Y.-H. Lin and S.-H. Shao, Anomalies and bounds on charged operators, *Phys. Rev. D* **100**, 025013 (2019), [arXiv:1904.04833](#).
- [99] P. Di Francesco, P. Mathieu, and D. Senechal, *Conformal Field Theory*, Graduate Texts in Contemporary Physics (Springer-Verlag, New York, 1997).
- [100] P. Ginsparg, *Applied conformal field theory* (1988), [arXiv:hep-th/9108028 \[hep-th\]](#).
- [101] A. Vishwanath and T. Senthil, Physics of three-dimensional bosonic topological insulators: Surface-deconfined criticality and quantized magnetoelectric effect, *Phys. Rev. X* **3**, 011016 (2013).
- [102] C. Xu and T. Senthil, Wave functions of bosonic symmetry protected topological phases, *Physical Review B* **87**, 10.1103/physrevb.87.174412 (2013).
- [103] Z. Bi, A. Rasmussen, K. Slagle, and C. Xu, Clas-

- sification and description of bosonic symmetry protected topological phases with semiclassical nonlinear sigma models, *Physical Review B* **91**, [10.1103/physrevb.91.134404](#) (2015).
- [104] I. Affleck and F. D. M. Haldane, Critical theory of quantum spin chains, *Phys. Rev. B* **36**, 5291 (1987).
  - [105] X. Chen, Z.-X. Liu, and X.-G. Wen, Two-dimensional symmetry-protected topological orders and their protected gapless edge excitations, *Phys. Rev. B* **84**, 235141 (2011), [arXiv:1106.4752](#).
  - [106] V. L. Pokrovsky and A. L. Talapov, Ground state, spectrum, and phase diagram of two-dimensional incommensurate crystals, *Physical Review Letters* **42**, 65 (1979).
  - [107] M. Oshikawa, M. Yamanaka, and I. Affleck, Magnetization plateaus in spin chains: “haldane gap” for half-integer spins, *Physical Review Letters* **78**, 1984 (1997).
  - [108] K. Totsuka, Magnetization plateaus in spin chains — “haldane gap for half-integer spins” revisited, *Physical Review B* **57**, 3454 (1998).